AD-A053 349 AIR FORCE INST OF TECH WRIGHT-PATTERSON AFB OHIO SCH--ETC F/G 20/5
FIELD PROPERTIES OF MULTIPLE, COHERENTLY COMBINED LASERS.(U)
DEC 77 H E HAGEMEIER

UNCLASSIFIED AFIT/GEO/EE/77D-3 NL

1 OF 2
AD
A053349

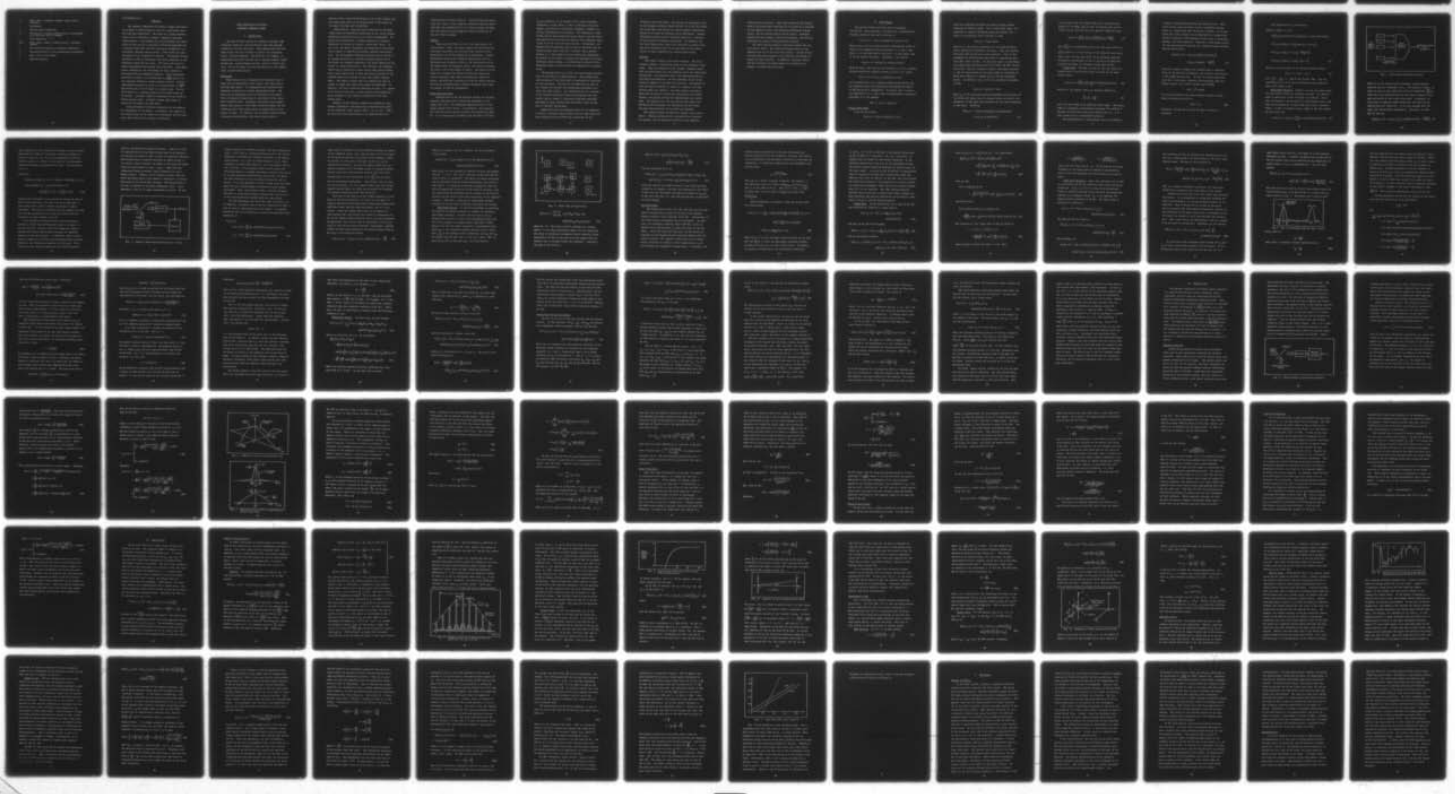

AFIT/GEO/EE/77D-3

FIELD PROPERTIES OF MULTIPLE, COHERENTLY COMBINED LASERS

THESIS

AFIT/GEO/EE/77D-3 Hal E. Hagemeier
Capt USAF

Approved for public release; distribution unlimited

(14) AFIT/GEO/EE/77D-3

(6) FIELD PROPERTIES OF MULTIPLE, COHERENTLY COMBINED LASERS.

(9) master's THESIS.

Presented to the Faculty of the School of Engineering

of the Air Force Institute of Technology

Air University

in Partial Fulfillment of the

Requirements for the Degree of

Master of Science

(12) 102 p.

by

(10) Hal E. Hagemeier, B.S.

Capt. USAF

Graduate Electrical Engineering

(11) Dec [redacted] 77

Approved for public release; distribution unlimited.

SECURITY CLASSIFICATION OF THIS PAGE (When Data Entered)

REPORT DOCUMENTATION PAGE		READ INSTRUCTIONS BEFORE COMPLETING FORM
1. REPORT NUMBER GEO/EE/77D-3	2. GOVT ACCESSION NO.	3. RECIPIENT'S CATALOG NUMBER
4. TITLE (and Subtitle) FIELD PROPERTIES OF MULTIPLE, COHERENTLY COMBINED LASERS		5. TYPE OF REPORT & PERIOD COVERED Master's thesis 6. PERFORMING ORG. REPORT NUMBER
7. AUTHOR(s) Hal E. Hagemeier Capt		8. CONTRACT OR GRANT NUMBER(s)
9. PERFORMING ORGANIZATION NAME AND ADDRESS Air Force Institute of Technology (AFIT-EN) Wright-Patterson AFB, Ohio 45433		10. PROGRAM ELEMENT, PROJECT, TASK AREA & WORK UNIT NUMBERS
11. CONTROLLING OFFICE NAME AND ADDRESS		12. REPORT DATE December 1977 13. NUMBER OF PAGES
14. MONITORING AGENCY NAME & ADDRESS(if different from Controlling Office) Air Force Avionics Laboratory (AFAL-DHO) Air Force Systems Command Wright-Patterson AFB, Ohio 45433		15. SECURITY CLASS. (of this report) Unclassified 15a. DECLASSIFICATION/DOWNGRADING SCHEDULE

16. DISTRIBUTION STATEMENT (of this Report)

Approved for public release; distribution unlimited

17. DISTRIBUTION STATEMENT (of the abstract entered in Block 20, if different from Report)

18. SUPPLEMENTARY NOTES

Approved for public release; IAW AFR 190-17

Jerral F. Guess, Captain, USAF
Director of Information

19. KEY WORDS (Continue on reverse side if necessary and identify by block number)

Lasers
Statistical Models
Ambiguity Function
Random Arrays

20. ABSTRACT (Continue on reverse side if necessary and identify by block number)

The coherent combination of several, single mode lasers can produce a field similar to that of a mode-locked laser but with more flexibility. The field for a quasi-monochromatic wave is considered a complex, coherence separable random process. The ensemble mean and covariance are determined for the case of a temporally stabilized amplitude and a temporal phase that with the appropriate assumptions is a stationary, gaussian random process. Mean fields are used

(continued on reverse)

DD FORM 1 JAN 73 1473 EDITION OF 1 NOV 65 IS OBSOLETE

$12.225

SECURITY CLASSIFICATION OF THIS PAGE (When Data Entered)

(continued from block 20)
throughout as the 'signals' of interest. The Huygens-Fresnel principle is used to investigate the field properties in the Fraunhofer region for two cases. The first case is for N beams superimposed with optical axes coincident. With appropriate assumptions, the performance of such a system is determined from the ambiguity function. Range measurement precision is found to be proportional to $1./\sqrt{N^3\Delta f}$ where Δf is the frequency difference between adjacent lasers. Velocity measurement precision is found to be proportional to $\sqrt{N\Delta f^2}$. The second case is for N beams in a linear array. The far field result is a scanning beam that in certain cases can be steered. Aperiodic arrays are considered in an effort to reduce grating lobes. An array of about 1000 lasers is needed for reasonably low side lobes.

Some generalized results are presented for the effects of misalignment of the lasers. In addition, the effects of the random phases of the lasers are considered, and the time-space dual nature of the results is discussed.

(Ncubed x deltaf) to the 1/2 power

Preface

This study has been a very interesting and useful learning experience, and I wish to convey my appreciation to the Air Force Institute of Technology for requiring it and to the Air Force Avionics Laboratory for the subject matter. I found that not only is coherent combination of lasers a formidable engineering task, it is equally as difficult to model the problem on paper. This is in part because of the cross talk between the disciplines of Electrical Engineering and Laser Physics, but the effort broadened (pressure broadening I believe) my understanding considerably.

I had hoped to be able to consider many more applications and in much greater detail, but there was, as usual, no time. I believe the results, however, to be significant, particularly in the array section where it was found that a very large number of lasers is needed to eliminate multiple lobes in the far field combined beam pattern. It was also found that, given a good phase locked loop, there are few major impediments to implementing a system of coherently combined lasers. This in itself is a useful result. There are however, many more questions to be answered, and I hope that this study can be a useful starting point for further efforts.

I want to express a great deal of thanks to my advisor, Dr. Stan Robinson, for his stimulating discussions. His expertise and understanding of the subject were invaluable.

I also want to thank my readers Dr. Ted Luke and Dr. Don Shankland for their very helpful comments. Last, but not least, I wish to thank my typists, Mrs. Karen Landis and Mrs. Rusti Gaudreau, who, though they are still probably wondering about all those funny little symbols, typed this report with great skill and care.

Hal E. Hagemeier
December 1977

Contents

List of Figures

Definition of Symbols

A	Field amplitude, sometimes indexed, always deterministic
a, b	Real and imaginary parts of $\tilde{q}$
B	Power ratio of threshold level to theoretical average side lobe level
D, d	Element spacings in an array, sometimes indexed, may be deterministic or random
E	Energy of signal s(t)
$\mathcal{F}_{xy}( )$	Two dimensional Fourier transform on the variables x, y
f_i	Frequency offset of ith laser
Δf	Constant frequency offset
f_o	Optical frequency
f_s	Scan frequency (rate)
g	Scale factor for linear frequency modulation
h	Peak spatial side lobe level with respect to the main beam
k	Propagation constant, $\frac{2\pi}{\lambda}$ (k is sometimes used as an index)
L	Length of laser array
m	Number of pulses
n	Array parameter
N	Number of lasers
N_o	Twice the height of the power spectral density of white noise
o_i	Misalignment angle of optic axis for the ith laser
$P(x_1,y_1)$	Phase factor from the Huygens-Fresnel principle
q	Logarithm (base 10) of L in wavelengths
$\tilde{q}$	Complex radius of curvature of gaussian spherical wave

r	Scale factor that determines the size of the scan sector
R	Radius of curvature of the phase front of a gaussian spherical wave
$R(\tau)$	Correlation of a random process, may be subscripted to indicate the particular process
$s(t)$	Signal of interest
$S(f)$	Fourier transform of $s(t)$
t_p	Temporal null-to-null pulse width
T_p	Temporal pulse recurrence interval
T_c	Coherence time of $\phi(t)$
U_o	Field at output of laser
U_{os}	Spatial part of U_o
U_1	Field at z_1
U_{1s}	Spatial part of U_1
w	Spot size of gaussian spherical wave
w_1	Spot size at z_1
x_p	Spatial null-to-null pulse width
X_p	Spatial period
z	Argument for z transforms
z_1	Distance beam propagates in z direction (no relation to z transforms)
α_x, α_y	Phase angles
β	Confidence level of B
γ	RMS bandwidth of $s(t)$
δ	RMS duration of $s(t)$ (no relation to the Dirac delta function)
ε	Difference between random variable and its mean
ζ	Beam angle in plane of array
η	Attenuation due to σ

θ	Phase angle, sometimes indexed, always deterministic
λ	Wavelength
ν	Doppler shift (frequency)
σ^2	Variance of a random quantity which is determined by a subscript, may be indexed
τ	Time difference, $t - t'$
$\phi(t)$	Phase angle, always a random process, sometimes indexed
Φ	Characteristic function, sometimes subscripted
χ	Ambiguity function (a two dimensional correlation)
ψ	Angle off of array normal
ω	Angular frequency

Abstract

The coherent combination of several, single mode lasers can produce a field similar to that of a mode-locked laser but with more flexibility. The field for a quasi-monochromatic wave is considered a complex, coherence separable random process. The ensemble mean and covariance are determined for the case of a temporally stabilized amplitude and a temporal phase that with the appropriate assumptions is a stationary, gaussian random process. Mean fields are used throughout as the "signals" of interest. The Huygens-Fresnel principle is used to investigate the field properties in the Fraunhofer region for two cases. The first case is for N beams superimposed with optical axes coincident. With appropriate assumptions, the performance of such a system is determined from the ambiguity function. Range measurement precision is found to be proportional to $\frac{1}{\sqrt{N^3 \Delta f}}$ where Δf is the frequency difference between adjacent lasers. Velocity measurement precision is found to be proportional to $\sqrt{N \Delta f^3}$. The second case is for N beams in a linear array. The far field result is a scanning beam that in certain cases can be steered. Aperiodic arrays are considered in an effort to reduce grating lobes. An array of about 1000 lasers is needed for reasonably low side lobes.

Some generalized results are presented for the effects of misalignment of the lasers. In addition, the effects of the random phases of the lasers are considered, and the time-space dual nature of the results is discussed.

FIELD PROPERTIES OF MULTIPLE, COHERENTLY COMBINED LASERS

I. Introduction

The uses of laser systems in industry, medicine, the scientific community, and the military have been growing steadily in the past few years. Many applications have utilized lasers that are scanned or pointed, have high peak powers, and are modulated. The military, for example, is developing lasers for possible use in ranging systems, target designators, terrain mapping systems, and fire control systems. One of the types of laser used belongs to the general class of mode-locked lasers.

Background

Mode-locking of an inhomogeneously broadened laser is often done in applications that require very short pulses and high peak powers. An inhomogeneously broadened laser typically oscillates at several longitudinal modes. The modes are at frequencies that are separated by an amount that is inversely proportional to the length of the cavity (Ref 33:348-352,365). Generally, these modes have random phases with respect to each other (relative phases) and the resultant total laser output power is proportional to the number of modes. If, however, the individual modes maintain a constant relative phase, the laser output power is

periodic with a period proportional to the cavity length, and the output peak power is now proportional to the square of the number of modes (Ref 39:256-262).

Unfortunately, since the pulse properties of the mode-locked laser are determined essentially by the cavity length, variations in pulse format are not easily accomplished. To obtain more flexibility, it seems reasonable to consider combining the outputs of several, single mode lasers. In this case, the phase, frequency, and amplitude of each laser can be chosen to synthesize desirable combined beam properties. If the frequency difference between any two lasers is an integer multiple of a constant frequency offset and if the fields are combined coherently, the result duplicates the output of a mode-locked laser. Now, however, the frequency offset can be varied over a much larger range than possible with a mode-locked laser so that the pulse properties of the combined beam can be chosen to meet more diverse requirements. The number of beams that are combined can also be varied to change the output pulse width and amplitude. In addition, the lasers could be separated in space, i.e. placed in an array of some sort, so that spatial pulse properties exist analagous to the temporal properties of the mode-locked laser.

Analysis of the coherent combination problem has been largely experimental and based only on deterministic models of the individual laser outputs (Ref 1, 16, 17, 41). There has also been some speculation on the applicability of a

"phased array" of lasers (Ref 7). Although these are necessary first steps, a more complete analytical approach which considers the instabilities of the various lasers and examines the resulting electromagnetic field distribution in the far field is needed.

Problem

This study will focus on two of the many aspects of this problem. First, the laser outputs will be modeled as stochastic processes, and the space-time electric field distribution of the far field will be determined. Second, performance criteria for potential applications will be determined and related not only to the characteristics of the lasers (such as frequency, phase, and spatial location), but also to the total number of lasers. The purpose of the study is to examine the effects of practical quantities such as coherence time, phase instabilities, number of lasers, and position inaccuracies on the far field beam pattern and to determine from a systems standpoint what types of signals can then be synthesized.

Scope and Assumptions

Although most of the calculations (except for specific numerical examples) will be generally applicable to any single mode laser, the underlying application will be for carbon dioxide (CO_2) lasers. In particular, the waveguide CO_2 laser possesses certain desirable characteristics (Ref 9): it is homogeneously broadened and therefore oscillates

at one frequency; it is tuneable over a large frequency bandwidth; as a CO_2 laser, it has a relatively long wavelength; and there is a convenient atmospheric "window" at the CO_2 wavelength of 10.6 microns. For simplicity, scalar fields will be used instead of vector fields, and the field descriptions will be classical (such as the treatments found in Ref 12:37-50; 14:11-26; and 4:10-36). Furthermore, the Huygens-Fresnel principle will be used to determine the far field patterns (Ref 4:370-375; 12:33-70), and a perfect channel (i.e. free space) will be assumed for propagation. No attempt will be made to consider the problems of actually combining, phase locking, or controlling the phases of the individual beams as these topics are addressed in a related study.

The desired result is a first and second moment description of the field as a random process. The ensemble mean and covariance of the field will be considered as functions of time and space. The mean of the field will be used as the "signal" of interest for determining performance criteria and other results. The covariance will be a measure of how closely the actual results will approach the mean results and is similar to the mutual coherence functions described by other authors (Ref 4:499-518; 3:765; 21:235-242; 27:359-399; 29:784-789).

Signal detection and estimation will not be addressed in detail; desirable signal formats will be those which produce workable patterns within the constraints of the

stochastic far field model. One measure of performance will be the ambiguity function (Ref 6:59-105; 31:70-75) from which the Cramer-Rao lower bounds on a given signal's measurement precision of range and velocity can be determined. Another performance measure will be the beam quality as a function of laser position and phase variations. In addition, the far field beam pattern itself as a function of various time and space conditions will be an indication of the desirability of those conditions for certain applications.

Approach

The study is divided into three sections. The first section presents a statistical model of the individual laser modes. They are considered to be complex, coherence separable processes whose real and imaginary parts are identically distributed. For practical cases, the mode amplitudes are considered deterministic, and the randomness (laser instabilities) appears in the phase of each beam. The duality of time and space variations is shown as a general case when several beams are combined. Far field results are determined and the effects of physical limitations are studied. Finally, two general classes of combined beams are considered: the coaxial case, and the side-by-side array case. The means and covariances are determined for both cases, and some characteristics of the means are examined.

The second section considers the coaxial case in more detail. Coherent detection and a matched filter receiver are assumed, and the ambiguity function of the combined

field mean is determined. This shows explicitly the dependence of the measurement precision of the signal as a function of the number of lasers, the frequency differences between lasers, and the relative phases of the lasers. Potential applications for ranging, velocity measurement, and both are considered in light of the performance criteria.

The third section presents analytical results for various linear arrays. The scanning characteristics of the combined beam in the far field are studied. Pattern synthesis and other beam properties are related to the number of lasers and their position. In addition, aperiodic arrays and the statistics of random arrays are included in an attempt to reduce high side lobes.

II. Field Models

The optical fields used here will be described classically. Most generally, the field for a monochromatic linearly polarized wave may be written as

$$u(x,y,z,t) = A(x,y,z,t)\cos\left[2\pi f_0 t - \phi(x,y,z,t)\right]$$

where $u(x,y,z,t)$ is a scalar function representing either an electric or a magnetic field at position x, y, and z, and time t; A is the amplitude of the wave; ϕ is the phase; and f_0 is the optical frequency. Typically, u is written

$$u(x,y,z,t) = \mathrm{Re}\left[U(x,y,z,t)\exp(-j2\pi f_0 t)\right]$$

where Re means "the real part of" and $U(x,y,z,t)$ is a complex function called the complex envelope of $u(x,y,z,t)$, where

$$U(x,y,z,t) = A(x,y,z,t)\exp\left[j\phi(x,y,z,t)\right]$$

It is assumed that U is a complex random process whose real and imaginary parts are identically distributed and that z is the direction of propagation. The field, then, at any z is a function of x, y, and t and is designated by a numerical subscript on U, for example

$$U(x,\ y,\ z_0,t) = U_0(x,y,t)$$

Output Field Model

U can now be written

$$U(x,y,t) = A(x,y,t)\exp\left[j\phi(x,y,t)\right]$$

where the amplitude and phase are slowly varying random functions of time and space. For a single mode laser, the amplitude is usually considered spatially coherent for a given z and separable (Ref 3:768,770) so that

$$A(x,y,t) = A_s(x,y)A(t)$$

where A_s is the spatial dependence of the field amplitude and is generally considered to be known. (The last section will deal with results for x and y unknown.) A(t) is the randomness of the amplitude due mostly to spontaneous emission (Ref 3:765; 21:236). If the laser output is considered to be amplitude stabilized (Ref 2:32; 18:378; 28:2399; 29:784; and 33:63), then A(t) becomes a simple, non-random constant, A, and the fluctuations of the laser light are primarily in phase (the effect of a random $A_s(x,y)$ will be considered later). In addition, $\phi(x,y,t)$ is also considered separable so that

$$\phi(x,y,t) = \phi_s(x,y) + \phi(t)$$

where ϕ_s is the non-random spatial dependence of the phase of the field (the random case is treated later) and $\phi(t)$ is the randomness of the phase that accounts for the line broadening of the laser. Therefore,

$$U(x,y,t) = A\{A_s(x,y)\exp[j\phi_s(x,y)]\}\exp[j\phi(t)]$$

$$= A\, U_s\,(x,y)\, \exp[j\phi(t)] \qquad (1)$$

It is assumed that the single mode lasers discussed here operate in the TEM_{oo} mode so that the spatial part of the field, $U_s(x,y)$, has the form of a gaussian spherical wave,

$$U_s(x,y) = \sqrt{\frac{2}{\pi}}\,\frac{1}{w}\,\exp\left[-j\left(\frac{\pi}{\lambda}\right)\frac{x^2+y^2}{R}\right]\exp\left[-\frac{x^2+y^2}{w^2}\right] \qquad (2)$$

where $\sqrt{\frac{2}{\pi}}\,\frac{1}{w}$ is a normalizing factor for unit power flow (i.e. $\int_{-\infty}^{\infty}\int|U_s|^2dxdy=1$), R is the radius of the spherical wave phase front, and w is the "spot size" of the gaussian amplitude distribution (equivalent to the e^{-1} point or $\sqrt{2}$ times the standard deviation of a gaussian curve) (Ref 33:307).

Single Beam. From Eqs (1) and (2) for the output of a single laser at some initial plane in front of the laser output mirror,

$$U_0(x,y,t) = \sqrt{\frac{2}{\pi}}\,\frac{1}{w}\,\exp\left[-j\frac{\pi}{\lambda\tilde{q}}(x^2+y^2)\right]A\exp\left[j(\theta+\phi(t))\right] \qquad (3)$$

where $\tilde{q}$ is the complex radius of curvature defined by

$$\frac{1}{\tilde{q}} = \frac{1}{R} - j\frac{\lambda}{\pi w^2} \qquad (4)$$

and θ has been added as an arbitrary phase angle. This phase angle is considered a controllable parameter (it could be a function of time) which will prove useful later on. A is also assumed to be a controllable quantity.

The random phase of a free-running laser is ultimately

a result of spontaneous emission and quantum noise. These noise sources cause the phase to be a stochastic process known as a random walk (Ref 18:370-371; 34:181). It is well known that such a process can be described as a Wiener-Lévy process (sometimes called Brownian motion) that is zero mean, gaussian, and non-stationary. Therefore, using known results for the characteristic function of a gaussian random variable (Ref 26:254,474-510),

$$E\{U_0(x,y,t)\} = AU_{0S}(x,y)E\left\{\exp\{j[\theta+\phi(t)]\}\right\}$$

$$= AU_{0S}(x,y)\exp\left(j\theta - \frac{\sigma^2(t)}{2}\right) \qquad (5)$$

where $E(\ )$ means to compute the ensemble mean or expected value of the quantity in brackets, and $\sigma^2(t)$ is the variance of the random process $\phi(t)$. If $n(t)$ is a white noise process that is zero mean, gaussian, and stationary then the Weiner process, $\phi(t)$ can be written (Ref 26:502),

$$\phi(t) = \int_0^t n(u)du$$

If α is the height of the power spectral density of $n(t)$, then the variance of $\phi(t)$ is,

$$\sigma^2(t) = \alpha t \qquad (5a)$$

Therefore, the mean of U_0 in Eq (5) goes to zero as t increases.

The correlation of U_0 now becomes

$$E\left(U_0(x,y,t)U_0^*(x',y',t')\right)$$

$$=E\left\{AU_{0_S}(x,y)\exp\{j[\theta+\phi(t)]\}AU_{0_S}^*(x',y')\exp\{-j[\theta+\phi(t')]\}\right\}$$

$$=A^2U_{0_S}(x,y)U_{0_S}^*(x',y')E\left\{\exp\{j[\phi(t)-\phi(t')]\}\right\}$$

$$=A^2U_{0_S}(x,y)U_{0_S}^*(x',y')\exp\left(-\frac{\sigma_\Delta^2(t,t')}{2}\right)$$

$$=A^2U_{0_S}(x,y)U_{0_S}^*(x',y')\exp\left(-\frac{\alpha}{2}|t-t'|\right) \qquad (6)$$

where σ_Δ^2 is the variance of the gaussian random process

$$\Delta\phi(t,t') = \phi(t) - \phi(t') \qquad (7)$$

and $-\frac{\sigma_\Delta^2}{2} = -\frac{\alpha}{2}|t-t'|$ (Ref 8:139; 26:476, 502). Now the correlation of U_0 in Eq (6) is stationary even though the phase $\phi(t)$ itself is not.

Multi-Beam (Coaxial). Figure 1 (on the next page) shows the case where N beams are combined coaxially. No consideration is given here to how the beams are combined. Since this investigation was motivated by a mode-locked laser, each mode can be modeled by a single mode laser with a frequency offset, so that a frequency term is added to the time dependent part of Eq (3),

$$U_0(x,y,t) = U_{0_S}(x,y)\sum_{i=0}^{N-1} A_i \exp\{j[2\pi f_i t+\theta_i+\phi_i(t)]\} \qquad (8)$$

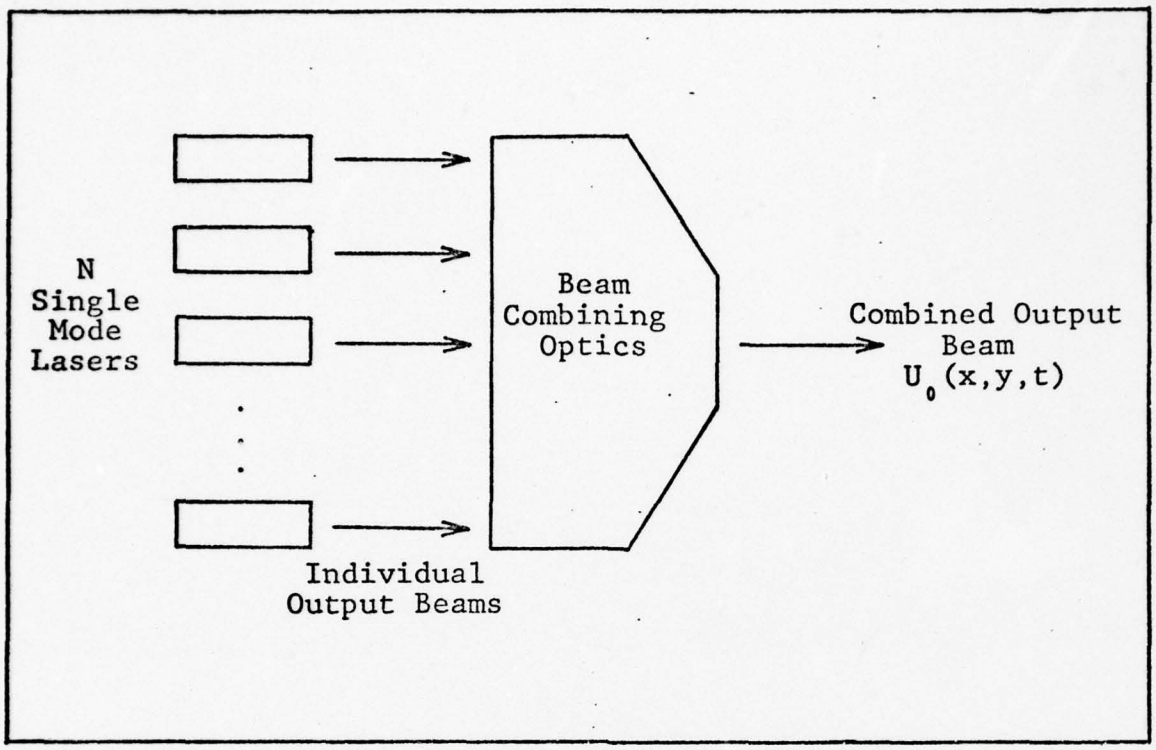

Fig. 1. Multi-Beams Combined Coaxially

where f_i is the (controllable) frequency spacing between adjacent spectral components of U_0. The number of lasers, N, that are used is only limited by the total bandwidth, $\sum_{i=0}^{N-1} f_i$, since the total bandwidth must be less than or equal to the gain line width of the lasers being used. In general, f_i could have an additive random component, but this will be ignored here for simplicity. It is also assumed that the $\phi_i(t)$ are statistically independent. Therefore, as with Eqs (3) and (5),

$$E\left[U_0(x,y,t)\right] = U_{0s}(x,y) \sum_i A_i \exp\left[j(2\pi f_i t+\theta_i) - \frac{\sigma_i^2(t)}{2}\right] \quad (9)$$

where $\sigma_i^2(t)=\alpha_i t$ is the variance of the phase of the ith beam. This might be called an "open loop" expression (similar to Eq (5)) in that A_i, f_i, and θ_i are deterministic and unrelated to $\phi_i(t)$, i.e. there is no attempt to use measurement dependent feedback to compensate for $\phi_i(t)$. The covariance of U_0 is

$$\mathrm{Cov}[U_0, U_0']$$

$$= E[U_0(x,y,t)U_0^*(x',y',t')] - E[U_0(x,y,t)]E[U_0^*(x',y',t')]$$

$$= U_{0s}(x,y)U_{0s}^*(x',y') \sum_i A_i^2 \exp[j2\pi f_i(t-t')]$$

$$\{\exp\left[-\frac{\alpha_i}{2}|t-t'|\right] - \exp\left[-\frac{\alpha_i}{2}(t+t')\right]\} \qquad (10)$$

Although the covariance is non-stationary (since the mean of $\phi(t)$ is non-stationary), the last term in Eq (10) goes to zero quickly with t and t' and the covariance is quasi-stationary. The mean of the field in Eq (9) behaves as in Eq (5), and the covariance of U_0 in Eq (10) varies with the statistics of $\phi_i(t)$ similar to Eq (6).

It is possible to continue using the non-stationary statistics of the free-running phase $\phi_i(t)$ as is done in Eqs (9) and (10). However, this will render the results unusable for certain applications (notably the ambiguity function in the next section). In addition, there is presently no known way to measure such field quantities directly. Therefore, the following assumptions will be made: First, the mean of the field (as opposed to the field intensity)

will be considered the signal of interest. Second, it will be required that for the field of any laser to be observed at any point in space or time, it must be coherently detected. This necessitates a receiver structure as shown in Fig. 2. In general, with no control, the phase of the detected signal would be proportional to $\phi_i(t) - \phi_0(t)$. Since both are independent Wiener processes, their difference is also a Wiener process. However, if the control is used, then the local oscillator phase $\phi_0(t)$ becomes a function of a measurement made by the closed loop receiver. This measurement is, in turn, a function of the phase difference $\phi_i(t) - \phi_0(t)$. Therefore, $\phi_0(t)$ is no longer independent of $\phi_i(t)$. If the

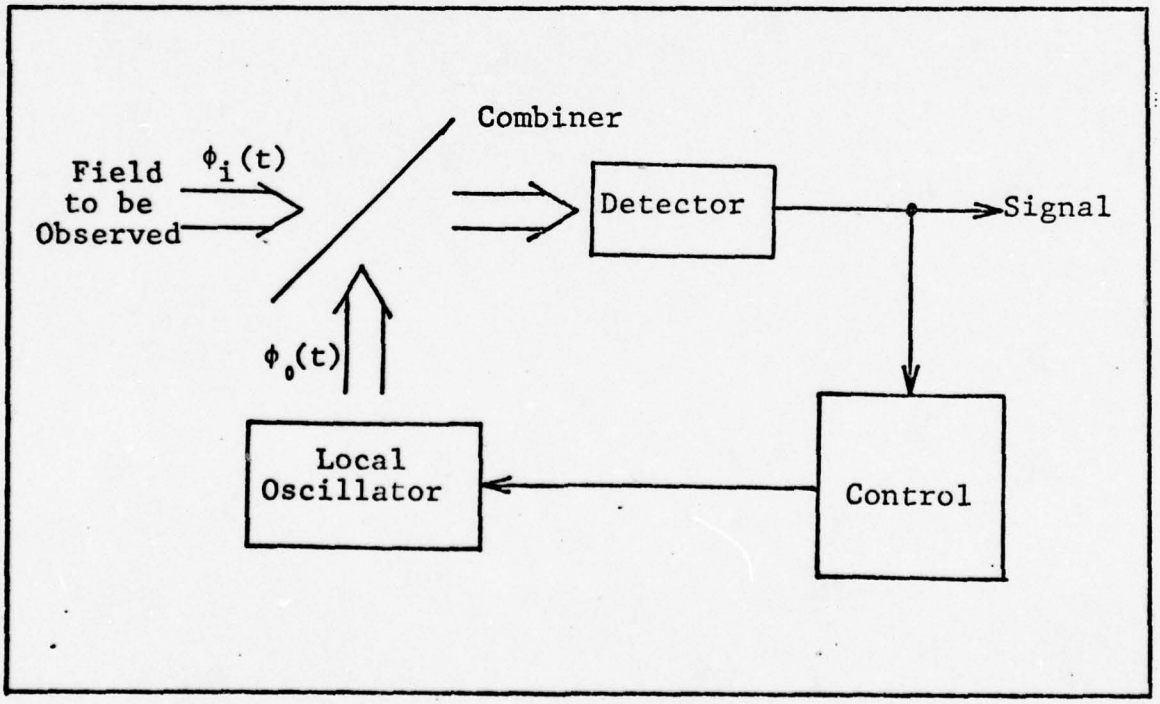

Fig. 2. Coherent (Heterodyne) Detection of a Field

control apparatus is properly designed, the phase difference $\phi_i(t) - \phi_0(t)$ will be a stationary process since the control mechanism is tracking the temporal variations of the differential phases, i.e. $\phi_0(t)$ is nearly locked to $\phi_i(t)$. (This assumption is often made implicity; see, for example, Ref 21: 237; 24:78,85.) In an absolute sense the two phases are still proceeding in a random walk manner, however, the receiver is only observing the difference between the two phases, and this difference can be controlled arbitrarily well in theory. It is not generally possible to make $\phi_0(t)$ precisely equal to $\phi_i(t)$ thereby making the observed signal totally non-random. Thus, the receiver of Fig. 2 usually produces non-exact or noisy phase control, wherein some, but not all, of the received field's instabilities are compensated.

For the multi-beam case in Eq (8), when the field is to be observed, a receiver such as the one illustrated by Fig. 2 must be used to coherently detect the signal. To simplify matters Eq (8) can be rewritten in terms of measureable field quantities as

$$U_0(x,y,t)$$

$$= U_{0s}(x,y) \sum_{i=0}^{N-1} A_i \exp\{j[2\pi f_i t+\theta_i+\phi_i(t)-\phi_0(t)]\}$$

$$= U_{0s}(x,y) \sum_{i=0}^{N-1} A_i \exp\{j[2\pi f_i t+\theta_i+\phi_i'(t)]\} \qquad (11)$$

where $\phi_i'(t)$ is defined to be the difference between the phase of the reference laser, $\phi_0(t)$, and the phase of the ith laser. If the phase of each laser is locked to the reference (similar to Fig. 2) then each of the $\phi_i'(t)$ in Eq (11) can be considered stationary. The use of a phase locked loop as a control mechanism will invariably change the gaussian random process $\phi_i(t)$ into a non-gaussian process $\phi_i'(t)$ such that $E\{\exp\{j\phi_i'(t)\}\}$ is not necessarily $\exp\left[-\frac{\sigma_i'^2}{2}\right]$ and the $\phi_i'(t)$ are not necessarily independent. Nevertheless, for the case of a strong signal, i.e. for a phase locked loop with a high signal-to-noise ratio, the $\phi_i'(t)$ may be modeled as independent gaussian random processes (Ref 38:86-92).

Since all of the lasers are now locked temporally to the phase of the local oscillator, the phase of the signal of interest becomes the controlled phase differences between the individual lasers and the local oscillator, and it is stationary. Hence the random walk nature of the phase of a free-running laser (or lasers) will always be transparent as far as any results derived from Eqs (8) or (11) are concerned. By definition, then, Eq (8) will be understood to have $\phi_i(t)$ $(=\phi_i'(t))$ that are zero mean, stationary, independent, gaussian random processes when observed in the required manner (Fig.2). The mean of the field now becomes

$$E\{U_0(x,y,t)\} = U_{0s}(x,y) \sum_i A_i \exp\left[j\{2\pi f_i t+\theta_i\} - \frac{\sigma_i^2}{2}\right] \qquad (12)$$

where the variance, σ_i^2, is a constant, and the covariance of U_0 becomes

$$\mathrm{Cov}(U_0, U_0') = U_{0s}(x,y)U_{0s}^*(x',y') \sum_i A_i^2 \exp\left(j2\pi f_i(t-t')\right)$$
$$\left\{\exp\left(-\sigma_i^2\right)\left(\exp\left(R\phi_i(\tau)\right)-1\right)\right\} \qquad (13)$$

where $R\phi_i(\tau)$ is the correlation function of $\phi_i(t)$ and depends only on $\tau = t-t'$. Now, σ_i^2 is a measure of how well the ith laser's phase is controlled. The degree of control necessary can be calculated based on system requirements (this will be done later). It should be noted that although Eqs (12) and (13) are apparently statistics of the field of interest, they are technically the statistics of the product of the field of interest and the field of the local oscillator in the required receiver. Since this assumption is always made, however, explicit use of the local oscillator field will not be used.

Multi-Beam (Array). It may not be possible or desirable for physical or economic reasons to combine the individual laser beams coaxially. In this case the lasers may be aligned side-by-side in a one or two dimensional array similar to the antennas in a phased array radar (Ref 7:1103). Figure 3 (on the next page) illustrates a rectangular array where D_{ik} is the (center-to-center) spacing in the x direction, d_{ik} is the spacing in the y direction, and D_{ik} and d_{ik} are larger than the spot size, w, for all i and k. Now, as shown in Eq (14) on the next page, the field becomes

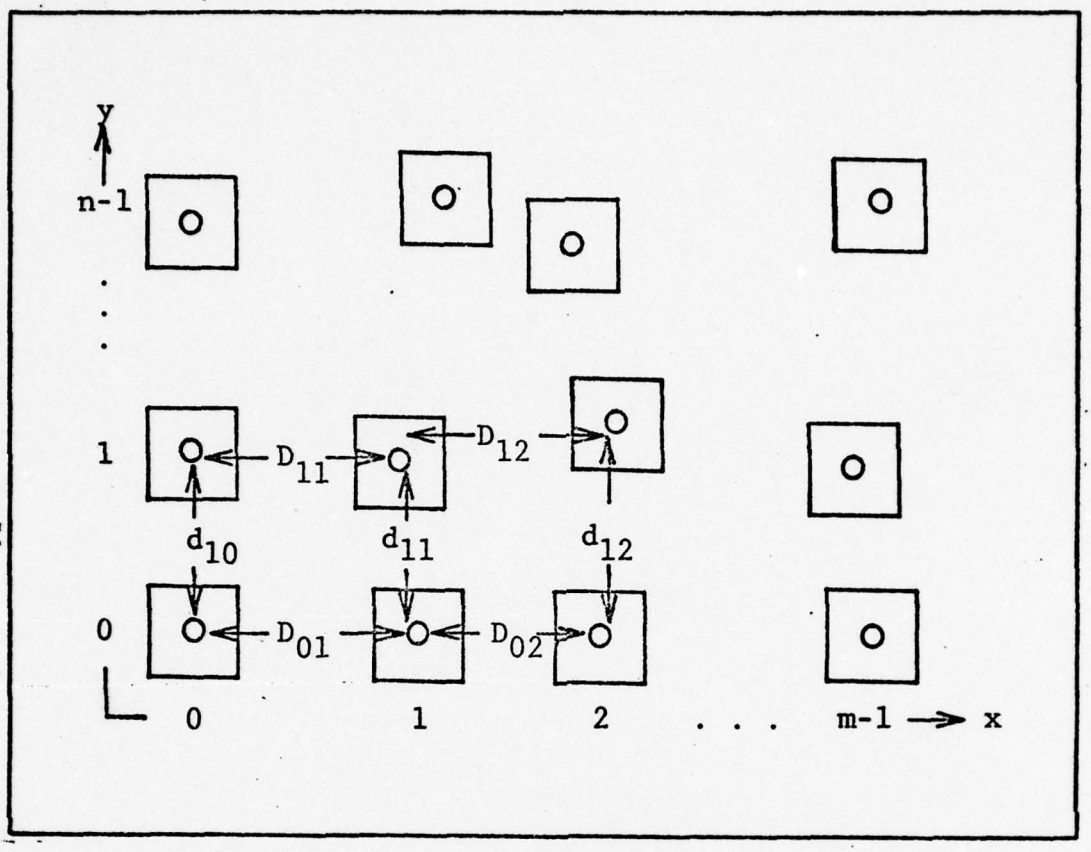

Fig. 3. Front View of Laser Array

$$U_0(x,y,t) = \sum_{i=0}^{n-1} \sum_{k=0}^{m-1} U_{0s}(x+D_{ik}, y+d_{ik})\, A_{ik}$$

$$\exp\{j(2\pi f_{ik}t+\theta_{ik}+\phi_{ik}(t))\} \qquad (14)$$

where mn = N. The lasers could be arranged in a circle, spiral, or any other geometrical shape, but for simplicity the array is considered rectangular unless otherwise noted. Essentially Eq (14) is the same as Eq (8) except that the spatial term is included within the summation. Similarly, the mean of the field is,

$$E\left(U_0(x,y,t)\right) = \sum_i \sum_k U_{0s}(x+D_{ik}, y+d_{ik})\, A_{ik}$$

$$\exp\left(j(2\pi f_{ik}t+\theta_{ik}) - \frac{\sigma_{ik}^2}{2}\right) \qquad (15)$$

and the covariance of U_0 is

$$Cov\left(U_0, U_0'\right) = \sum_i \sum_k U_{0s}(x+D_{ik}, y+d_{ik}) U_{0s}^*(x'+D_{ik}, y'+d_{ik})\, A_{ik}^2$$

$$\{\exp\left(j2\pi f_{ik}(t-t')\right)\}\{\exp\left(-\sigma_{ik}^2\right)\left(\exp\left(R\phi_{ik}(\tau)\right)-1\right)\} \qquad (16)$$

Since the spatial and temporal parts of the field have been assumed to be separate, the mean and covariance of the field in Eqs (15) and (16) behave the same with respect to $\phi_{ik}(t)$ as Eqs (12) and (13), i.e. only the spatial part of the field has been changed.

Far Field Model

The fields given in Eqs (3), (8), and (14) are now propagated through space by means of the well-known Huygens-Fresnel principle (Ref 4:370-375; 12:40-46). Interactions of the field with the atmosphere are not considered. In addition, the Fraunhofer condition (Ref 4:382-386; 12:61) is imposed since consideration is given here only for the far field. (Since the space and time parts of the fields are separate and the Huygens-Fresnel principle affects only the spatial function, the temporal results that will be determined, including the effects of the random process $\phi_i(t)$, are unchanged by propagation through space. If desired, the

fields could be determined in the near field using the Fresnel condition as in Ref 4:382-383. However, with little loss of generality, the Fraunhofer condition is used here for simplicity.) A sufficient condition for the Fraunhofer case requires that

$$z_1 >> \frac{\pi(x^2+y^2)_{max}}{\lambda} \tag{17}$$

This may be a rather stringent condition, for example, in the multi-beam array case where $(x+D_{ik})_{max}$ and $(y+d_{ik})_{max}$ may be on the order of 10 cm. Then if $\lambda = 10.6\mu$, z_1 must be about 600 m to be an order of magnitude larger than $\frac{\pi(x^2+y^2)_{max}}{\lambda}$.

After propagating a distance z_1 down the optical axis, the field becomes

$$U_1(x_1,y_1,t) = \frac{1}{j\lambda z_1} \exp\left(jkz_1\right)\exp\left(j\frac{k}{2z_1}(x_1^2+y_1^2)\right)\int_{-\infty}^{\infty}\int U_0(x,y,t)$$

$$\exp\left(-j\left(\frac{2\pi}{\lambda z_1}\right)(xx_1+yy_1)\right)dxdy$$

$$= P(x_1,y_1)\,\mathcal{F}_{xy}\left[U_0(x,y,t)\right] \tag{18}$$

where $P(x_1,y_1)$ is just the phase factor in front of the integral and $\mathcal{F}_{xy}(\ )$ is the two dimensional (spatial) Fourier transform of $U_0(x,y,t)$ on x and y (Ref 12:61). Although U_1 is considered a function of the rectangular coordinates

x_1 and y_1, it is also a function of the spatial frequencies f_x and f_y where $f_x = (x_1)/(\lambda z_1)$ and $f_y = (y_1)/(\lambda z_1)$ in keeping with the nature of the Fourier transform. In the following discussions, $U_0(x,y,t)$ is not considered to have an explicit aperture function limiting its spatial extent at the laser output. As noted in Ref 33:312-313, a conservative aperture design for maximum power transmission makes the aperture size about 3w (where w is the spot size of the beam). The diffraction effects of this aperture on the beam profile are completely negligible, hence there is no explicit dependence of U_1 on the aperture. Any other desired aperture function may be used and U_1 would become simply (though perhaps tediously) the spatial convolution of the Fourier transforms of $U_{0s}(x,y)$ and the desired aperture.

Single Beam. If the field of Eq (3) is used in Eq (18), the resulting far field for a single beam is

$$U_1(x_1,y_1,t) = P(x_1,y_1)\,\mathcal{F}_{xy}\{U_{0s}(x,y)\}A \exp\{j[\theta+\phi(t)]\} \quad (19)$$

The mean of the far field becomes

$$E\{U_1(x_1,y_1,t)\} = P(x_1,y_1)\,\mathcal{F}_{xy}\{U_{0s}(x,y)\}\,A \exp\left[j\theta-\frac{\sigma^2}{2}\right] \quad (20)$$

and the correlation becomes

$$E\{U_1(x_1,y_1,t)U_1^*(x_1',y_1',t')\} = P(x_1,y_1)P^*(x_1',y_1')U_{1s}(x_1,y_1) U_{1s}^*(x_1',y_1')\,A^2 \exp[-\sigma^2+R\phi(\tau)] \quad (21)$$

where $U_{1s}(x_1,y_1) = \mathcal{F}_{xy}\{U_{0s}(x,y)\}$. For completeness

$$\mathcal{F}_{xy}\{U_{0s}(x,y)\} = \mathcal{F}_x\{U_{0s}(x)\}\,\mathcal{F}_y\{U_{0s}(y)\}$$

$$= \sqrt{\frac{2}{\pi}}\,\frac{1}{w}\,\mathcal{F}_x\left\{\exp\left(-j\frac{\pi}{\lambda\tilde{q}}\,x^2\right)\right\}\mathcal{F}_y\left\{\exp\left(-j\frac{\pi}{\lambda\tilde{q}}\,y^2\right)\right\}$$

$$= \sqrt{\frac{2}{\pi}}\,\frac{-j\lambda\tilde{q}}{w}\,\exp\left\{j\,\frac{\pi\tilde{q}}{\lambda z_1^2}\,(x_1^2+y_1^2)\right\} \qquad (22)$$

From Eq (20),

$$P(x_1,y_1)\,\mathcal{F}_{xy}\{U_{0s}(x,y)\}$$

$$= -\sqrt{\frac{2}{\pi}}\,\frac{\tilde{q}\,\exp(jkz_1)}{wz_1}\,\exp\left\{j\,\frac{\pi}{\lambda z_1^2}(\tilde{q}+z_1)(x_1^2+y_1^2)\right\} \qquad (23)$$

and from Eq (21),

$$P(x_1,y_1)P^*(x_1',y_1')U_{1s}(x_1,y_1)U_{1s}^*(x_1',y_1')$$

$$= \frac{2\tilde{q}\tilde{q}^*}{\pi w^2 z_1^2}\,\exp\{j\,\frac{\pi}{\lambda z_1^2}[(\tilde{q}+z_1)(x_1^2+y_1^2)-(\tilde{q}^*+z_1)(x_1'^2+y_1'^2)]\} \qquad (24)$$

The intensity of this single beam in the far field is

$$I_1 = U_1(x_1,y_1,t)U_1^*(x_1,y_1,t)$$

$$= \frac{2(a^2+b^2)}{\pi w^2 z_1^2}\,A^2\,\exp\left\{-\frac{2\pi b}{\lambda z_1^2}\,(x_1^2+y_1^2)\right\} \qquad (25)$$

where from Eq (4) $\tilde{q}$ has the form $a + jb$ where

$$a = \frac{z_1(\pi w^2)^2}{(\pi w^2)^2+(\lambda z_1)^2} \quad , \quad b = \frac{\pi\lambda(wz_1)^2}{(\pi w^2)^2+(\lambda z_1)^2}$$

and in the far field case $R \simeq z_1$. In Eq (25) the far field intensity of the single beam is completely deterministic since so far the randomness has been assumed to be only in phase.

Multi-Beam (Coaxial). Again, the extension can be made to sum N beams and the far field now shows some interesting properties. $U_1(x_1,y_1,t)$ in this case can be determined either by adding N versions of Eq (19) with the appropriate addition of a frequency offset, f_i, or by applying the Huygens-Fresnel principle to Eq (8). The same result is obtained in either case,

$$U_1(x_1,y_1,t) = P(x_1,y_1)U_{1S}(x_1,y_1) \sum_i A_i \exp\{j[2\pi f_i t+\theta_i+\phi_i(t)]\} \quad (26)$$

The mean of this far field is

$$E[U_1(x_1,y_1,t)] = P(x_1,y_1)U_{1S}(x_1,y_1) \sum_i A_i \exp\left[j(2\pi f_i t+\theta_i)- \frac{\sigma_i^2}{2}\right] \quad (27)$$

The covariance is

$$Cov[U_1,U_1'] = P(x_1,y_1)P^*(x_1',y_1')U_{1S}(x_1,y_1)U_{1S}^*(x_1',y_1') \sum_i A_i^2 \exp[j2\pi f_i(t-t')]\{\exp[-\sigma_i^2](\exp[R\phi_i(\tau)]-1)\} \quad (28)$$

The intensity of this far field is not deterministic as it was for a single beam in Eq (25) because of the cross terms between beams. The mean of the intensity is

$$E(I_1) = \frac{2(a^2+b^2)}{\pi w^2 z_1^2} \exp\left(-\frac{2\pi b}{\lambda z_1^2}(x_1^2+y_1^2)\right)\left[\sum_i A_i^2 + \sum_{\substack{i=0 \\ i\neq k}}^{N-1}\sum_{k=0}^{N-1} A_i A_k \right.$$

$$\left. \exp\{j[2\pi(f_i-f_k)t+(\theta_i-\theta_k)] - \frac{\sigma_i^2+\sigma_k^2}{2}\}\right] \quad (29)$$

This is a somewhat formidable expression, but some minor simplifying assumptions later will make it more useful.

Examination of the mean in Eq (27) yields some interesting results. It is reasonable to assume that although the $\phi_i(t)$ are independent, the σ_i^2 are certainly similar if not identical. This is because of the nature of the noise sources producing the random phase fluctuations, because of the similarity of the phase locked loops, and because all of the lasers are assumed to be of the same type and construction. Also, since the A_i are controllable, they are assumed to be the same for convenience. Therefore, Eq (27) becomes

$$E(U_1(x_1,y_1,t)) = P(x_1,y_1)U_{1s}(x_1,y_1)A \exp\left(-\frac{\sigma^2}{2}\right)$$

$$\sum_i \exp(j(2\pi f_i t+\theta_i)) \quad (30)$$

At this point some assumptions must be made for f_i and θ_i so that a closed form solution can be obtained. If the frequencies between the lasers are all the same (as in a

mode-locked laser) then $f_i = i\Delta f$ where Δf is the constant frequency spacing. A similar assumption can be made for θ_i, but the results will not be affected in any significant or useful manner, so θ_i is considered zero. Now, Eq (30) becomes

$$E\{U_1(x_1,y_1,t)\} = P(x_1,y_1)U_{1s}(x_1,y_1)\,A \exp\left(-\frac{\sigma^2}{2} + j\left(\frac{N-1}{2}\right)2\pi\Delta ft\right)\frac{\sin N\pi\Delta ft}{\sin \pi\Delta ft} \quad (31)$$

The (sin Nx)/(sin x) term in Eq (31) (the typical result of a mode-locked laser as in Ref 39:131) is a pulse train in time as shown in Fig. 4. The pulses have a null-to-null

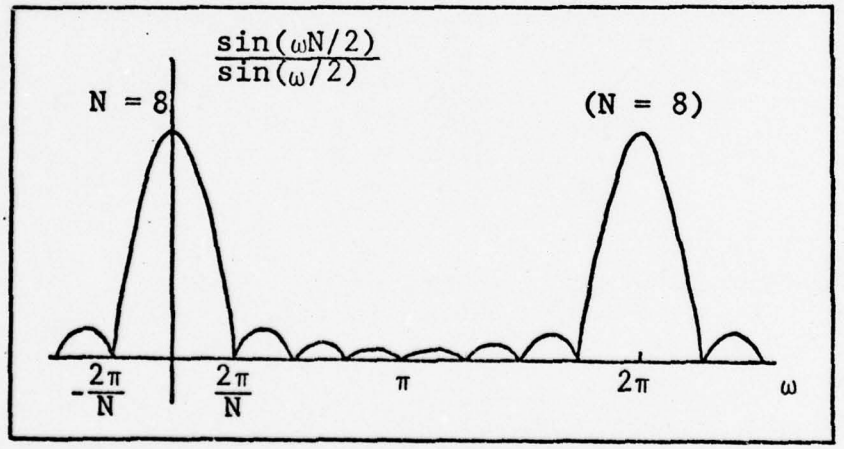

Fig. 4 Plot of $\sin(N\frac{\omega}{2})/\sin(\frac{\omega}{2})$ for N=8, $\omega=2\pi\Delta ft$

pulse width of

$$t_p = \frac{2}{N\Delta f} \quad (32)$$

and a pulse recurrence interval (pulse rate) of

$$T_p = \frac{1}{\Delta f} \quad (33)$$

For the waveguide CO_2 laser (whose gain line width is about 700 MHz), $N\Delta f$ must be less than or equal to 700 MHZ. Therefore the minimum achievable pulse width, t_p, is about 3 nsec. T_p depends on Δf which is limited by the total number of lasers used. The peak amplitude of the (sin Nx)/(sin x) function at each T_p is just N as expected for coherent superposition of N sources. The pulse width and pulse rate both depend on N and Δf which are assumed to be under the operator's control. Eq (31) also shows that the apparent frequency of the field is changed to the optical frequency f_0 minus $(\frac{N-1}{2})\Delta f$. Ref 41 reports experimental results of Eq (31).

If the assumptions for Eq (31) are applied to the intensity then the series terms in Eq (29) become

$$\sum_i A_i^2 = A^2 N$$

and

$$\sum_{i\neq k}\sum A_i A_k \exp\{j[2\pi(f_i-f_k)t+(\theta_i-\theta_k)] - \frac{\sigma_i^2+\sigma_k^2}{2}\}$$

$$= A^2 \exp(-\sigma^2) \sum_{i\neq k}\sum \exp[j(i-k)2\pi\Delta ft]$$

$$= A^2 \exp(-\sigma^2)\{\sum_i (N-i)(\exp[j2\pi\Delta fti]+\exp[-j2\pi\Delta fti])\}$$

$$= A^2 \exp(-\sigma^2)\{2\sum_i (N-i)\cos[i(2\pi\Delta ft)]\}$$

$$= A^2 \exp(-\sigma^2)\left[\frac{1-\cos N2\pi\Delta ft}{2\sin^2 \pi\Delta ft} - N\right]$$

$$= A^2 \exp(-\sigma^2)\left[(\frac{\sin N\pi\Delta ft}{\sin \pi\Delta ft})^2 - N\right]$$

(See Ref 22:104-105 for series sums.) Therefore,

$$E(I_1) = \frac{2(a^2+b^2)}{\pi w^2 z_1^2} \exp\left(-\frac{2\pi b}{\lambda z_1^2}(x_1^2+y_1^2)\right) A^2$$

$$\left((1-\exp(-\sigma^2))N + \exp(-\sigma^2)\left(\frac{\sin N\pi\Delta ft}{\sin \pi\Delta ft}\right)^2\right) \qquad (34)$$

If $\sigma^2 \to \infty$, $\exp(-\sigma^2) \to 0$ and $E(I_1)$ becomes a constant with respect to time. This is equivalent to the result of a multi-mode laser with no mode-locking. If $\sigma^2 \to 0$, $\exp(-\sigma^2) \to 1$ and $E(I_1)$ is a pulse train, i.e. $E(I_1) \to |E(U_1(x_1, y_1, t))|^2$ for $\sigma^2 \to 0$. This is equivalent to a mode-locked laser output.

The random phase fluctuations $\phi_i(t)$ simply cause the amplitude of the mean of the field in Eq (31) to be reduced by $\exp\left(-\frac{\sigma^2}{2}\right)$. As the variations in $\phi_i(t)$ become larger, the amplitude of the pulses in the far field becomes smaller. From this relation, the degree of control of the phases of the lasers can be calculated. If the desired maximum attenuation is η, then

$$\sigma = \sqrt{-2 \ln \eta} \qquad (35)$$

For example, if η is desired to be no larger than 1 db (about 0.80) then σ must be about 0.67 rad. Similarly, for phase control on the order of 1 rad, η is about 50%. The effect of $\phi_i(t)$ becomes even clearer upon examination of the total power flow through the $z = z_1$ plane. The mean power flow is

$$E(\text{Power}) = E\left(\int_{-\infty}^{\infty}\int |U_1(x_1, y_1, t)|^2 dx_1 dy_1\right)$$

$$E(\text{Power}) = \int_{-\infty}^{\infty}\int E(I_1)\,dx_1\,dy_1$$

Since $U_{0_S}(x,y)$ is already normalized for unit power flow (Eq (2)) and the Huygens-Fresnel principle merely changes the distribution of the power, not the amount, the mean power is

$$E(\text{Power}) = A^2\left[(1-\exp(-\sigma^2))N+\exp(-\sigma^2)\left(\frac{\sin N\pi\Delta ft}{\sin \pi\Delta ft}\right)^2\right]$$

Therefore, at t = 0 (pulse peak) and for A = 1,

$$E(\text{Power}) = (1-\exp(-\sigma^2))N + \exp(-\sigma^2)N^2 \qquad (36)$$

As $\sigma^2\to\infty$, E(Power) approaches N (incoherent superposition) and as $\sigma^2\to 0$, E(Power) approaches N^2 (coherent superposition).

It is also instructive to examine the behavior of the covariance of U_1 in Eq (28). For $\sigma_i = \sigma$,

$$\text{Cov}(U_1,U_1') \propto \exp(-\sigma^2)(\exp(R\phi(\tau))-1) \qquad (37)$$

The general characteristics of $R\phi(\tau)$ are that $R\phi(0) = \sigma^2$ and that $R\phi(\tau) = R\phi(-\tau)$, $R\phi(0) \geq |R\phi(\tau)|$, and generally $R\phi(\tau)\to 0$ as $\tau\to\infty$ (since $\phi_i(t)$ are zero mean processes) (Ref 23:126; 26:336-338). At $\tau = 0$, the covariance of U_1 becomes the variance, σ_u^2, of U_1 and

$$\sigma_{u1}^2 \propto 1-\exp(-\sigma^2) \qquad (38)$$

By the Chebyshev inequality (Ref 26:150) the probability that a random variable differs from its mean by more than an amount ε is less than or equal to its variance divided by ε^2.

Therefore,

$$\Pr\left(|U_1 - E(U_1)| \geq \varepsilon\right) \leq \frac{\sigma_u^2}{\varepsilon^2} \propto \frac{1-\exp(-\sigma^2)}{\varepsilon^2}$$

Now as $\sigma^2 \to 0$, $\Pr\left(|U_1 - E(U_1)| \geq \varepsilon\right)$ approaches zero, and U_1 is equal to its mean with probability one, i.e. the smaller the variance of $\phi_i(t)$, the more closely the field approaches its mean in Eq (27).

As $\tau \to \infty$, the two sample functions $\phi(t)$ and $\phi(t')$ become more and more uncorrelated. Typically, $R\phi(\tau) = 0$ for all $\tau \geq T_c$ where T_c is called the coherence time of the process $\phi(t)$. For time differences τ larger than the coherence time, the phases at the two times are uncorrelated. From Eq (37), $\tau > T_c$ implies that

$$\mathrm{Cov}\left(U_1, U_1'\right) = 0$$

i.e. the coherence time of the phase $\phi(t)$ is the coherence time of the field U_1. In general, $\mathrm{Cov}\left(U_1, U_1'\right)$ will decrease faster with τ than will $R\phi(\tau)$ so that the effective coherence time of U_1 may be less than that for $\phi(t)$, however, this is less true as $\sigma^2 \to 0$ (Ref 13:66). The coherence length of the field is related to the coherence time by the speed of light. (A longer coherence time implies a greater coherence distance.) Therefore, field points separated by times (distances) greater than the coherence time (distance) are uncorrelated.

One further comment on Eq (27) concerns the beam waist. Since the individual beams are added coaxially, the waist of

the total beam propagates as the waist of any single beam. Therefore, the waist w_1 at a distance z_1 is

$$w_1 \simeq \frac{\lambda z_1}{\pi w} \tag{39}$$

where w is the waist at $z = z_0$ (Eq (2)), and the far field here implies $z_1 >> \frac{\pi w^2}{\lambda}$ (Ref 33:308). For example, if w = 1mm and $\lambda = 10.6\mu$, then $z >> 0.3$ m which is a much less stringent condition than the Fraunhofer condition of Eq (17). Therefore, Eq (39) is essentially an equality when the Fraunhofer condition is met.

Multi-Beam (Array). For this case, Eq (26) becomes

$$U_1(x_1,y_1,t) = \sum_i \sum_k P(x_1,y_1)\, \mathcal{F}_{xy}\{U_{0s}(x+D_{ik},y+d_{ik})\}A_{ik}$$
$$\exp\{j\{2\pi f_{ik}t+\theta_{ik}+\phi_{ik}(t)\}\} \tag{40}$$

where as in Eq (14), mn = N. As in Eq (22),

$$\mathcal{F}_{xy}\{U_{0s}(x+D_{ik},y+d_{ik})\}$$
$$= \mathcal{F}_x\{U_{0s}(x+D_{ik})\}\, \mathcal{F}_y\{U_{0s}(y+d_{ik})\}$$
$$= \exp\left\{j\left(\frac{2\pi}{\lambda z_1}\right)x_1 D_{ik}\right\} \mathcal{F}_x\{U_{0s}(x)\} \exp\left\{j\left(\frac{2\pi}{\lambda z_1}\right)y_1 d_{ik}\right\} \mathcal{F}_y\{U_{0s}(y)\}$$
$$= \sqrt{\frac{2}{\pi}}\, \frac{-j\lambda\tilde{q}}{w} \exp\{j\left[\frac{\pi\tilde{q}}{\lambda z_1^2}(x_1^2+y_1^2)+\frac{2\pi}{\lambda z_1}(D_{ik}x_1+d_{ik}y_1)\right]\} \tag{41}$$

where the shifting theorem of Fourier transforms has been used (Ref 12:9; 27:65). Now Eq (40) can be written

$$U_1(x_1,y_1,t) = P(x_1,y_1)U_{1s}(x_1,y_1) \sum_i \sum_k A_{ik} \exp\{j[2\pi f_{ik}t_s+\theta_{ik}+\phi_{ik}(t)]\} \quad (42)$$

This is identical to Eq (26), the field for the multi-beam coaxial case, except for t_s where t_s is dependent on time and space,

$$t_s = t + \frac{D_{ik}x_1}{f_{ik}\lambda z_1} + \frac{d_{ik}y_1}{f_{ik}\lambda z_1} \quad (43)$$

The mean of this field is similar to Eq (27)

$$E[U_1(x_1,y_1,t)] = P(x_1,y_1)U_{1s}(x_1,y_1) \sum_i \sum_k A_{ik} \exp\left[j(2\pi f_{ik}t_s+\theta_{ik}) - \frac{\sigma_{ik}^2}{2}\right] \quad (44)$$

and the covariance is similar to Eq (28)

$$Cov[U_1,U_1'] = P(x_1,y_1)P^*(x_1',y_1')U_{1s}(x_1,y_1)U_{1s}^*(x_1',y_1') \sum_i \sum_k A_{ik}^2 \exp[j2\pi f_{ik}(t_s-t_s')]\{\exp[-\sigma_{ik}^2)(\exp[R\phi_{ik}(\tau)]-1)\} \quad (45)$$

where t_s' is a function of t', x_1', and y_1'. The mean of this field's intensity is

$$E[I_1] = \frac{2(a^2+b^2)}{\pi w^2 z_1^2} \exp\left[-\frac{2\pi b}{\lambda z_1^2}(x_1^2+y_1^2)\right] E\left[\left|\sum_i \sum_k A_{ik} \exp\{j[2\pi f_{ik}t_s+\theta_{ik}+\phi_{ik}(t)]\}\right|^2\right] \quad (46)$$

For the general two dimensional array this expression and Eq (44) cannot be evaluated analytically without numerous assumptions. Eqs (44) and (45) are similar to Eqs (27) and (28) respectively with t replaced by t_s. Qualitatively, the two dimensional array produces a pulse train in the far field (there are still N different frequencies being added so the results of Eq (31) hold for $x_1 = y_1 = 0$ in Eq (44)). However, there will be some additional spatial modulation because of Eq (43).

Generalized Results and Duality

Eq (42) is the key to some very general and interesting results. In this equation, if f_{ik}, D_{ik}, and d_{ik} are considered independent random variables, then Eq (44) becomes

$$E\{U_1(x_1,y_1,t)\} = P(x_1,y_1)U_{1s}(x_1,y_1) \sum_i \sum_k A_{ik} \exp(j\theta_{ik})$$

$$\Phi_f(2\pi t)\Phi_D(2\pi\frac{x_1}{\lambda z_1})\Phi_d(2\pi\frac{y_1}{\lambda z_1})\Phi_\phi(1) \qquad (47)$$

where the Φ's represent the characteristic functions of the indicated random variables as functions of the indicated arguments (i.e. $\Phi_x(\alpha) = E\{\exp(j\alpha x)\}$ where x is a random variable) and Φ_ϕ is evaluated at 1. Now if f, D, d, and ϕ are gaussian (and stationary) with means f_{ik}, D_{ik}, d_{ik} and ϕ_{ik} and variances σ_f^2, σ_D^2, σ_d^2, and σ_ϕ^2 respectively, then Eq (47) becomes (see Ref 26:159),

$$E(U_1) = P\ U_{1s}\{\exp -\tfrac{1}{2}\left[(2\pi t)^2\sigma_f^2+(2\pi\frac{x_1}{\lambda z_1})^2\sigma_D^2+(2\pi\frac{y_1}{\lambda z_1})^2\sigma_d^2+\sigma_\phi^2\right]\}$$

$$\sum_i \sum_k A_{ik} \exp\{j(2\pi f_{ik}t_s+\theta_{ik}+\phi_{ik})\} \qquad (48)$$

It is also reasonable that $\sigma_f = 0$ (i.e. f is completely deterministic) and $\phi_{ik} = 0$ so that

$$E(U_1) = P\ U_{1s}\exp\{-\tfrac{1}{2}\left[(2\pi\frac{x_1}{\lambda z_1})^2\sigma_D^2+(2\pi\frac{y_1}{\lambda z_1})^2\sigma_d^2+\sigma_\phi^2\right]\} \sum_i \sum_k A_{ik}$$

$$\exp\left[j(2\pi f_{ik}t+\frac{2\pi D_{ik}x_1}{\lambda z_1}+\frac{2\pi d_{ik}y_1}{\lambda z_1}+\theta_{ik})\right] \qquad (49)$$

It should be noted that Eq (41) is still valid for D and d random variables because the Fourier transform is taken term by term and each D_{ik}, d_{ik} are just numbers (albeit part of a sample space). In addition, D, d, and $\phi(t)$ are considered to have identical variances for each i, k as was assumed for Eq (30).

Now, Eq (49) is a useful general result. If $i = k = \sigma_D = \sigma_d = D_{ik} = d_{ik} = f_{ik} = 0$ the result is the single beam case represented by Eq (20) with $A_{oo} = A$ and $\theta_{oo} = \theta$. If $\sigma_D = \sigma_d = D_{ik} = d_{ik} = 0$ the result is the coaxial case represented by Eq (30) with $A_{ik} = A$, $f_{ik} = f_i$, and $\theta_{ik} = \theta_i$ (i.e. the double series collapses to a single series). If $\sigma_D = \sigma_d = 0$ the result is the general two dimensional array case with D_{ik} and d_{ik} deterministic as represented by Eq (44) (with $\sigma_{ik} = \sigma_\phi$).

If k = 0, the result is the general one dimensional linear array

$$E\left(U_1(x_1,y_1,t)\right) = P(x_1,y_1)U_{1S}(x_1,y_1)\exp\left\{-\tfrac{1}{2}\left((2\pi\frac{x_1}{\lambda z_1})^2\sigma_D^2+\sigma_\phi^2\right)\right\}$$

$$\sum_i A_i \exp\left(j(2\pi f_i t+ \frac{2\pi D_i x_1}{\lambda z_1} +\theta_i)\right) \quad (50)$$

The deterministic version of this field ($\sigma_D = 0$) will be treated in the last section as well as the case for D a random variable.

At this point, three sources of error in the far field that are a result of the physical positioning of the laser elements must be considered. These are errors in the element location in x (for a linear array, x and y for a planar array), errors in the alignment of the individual optical axes with each other, and errors in the element location in z. The first problem can be considered in a manner completely analagous to the results for the phase variance discussed in connection with Eqs (34), (35), and (36). For the linear array, each laser may have an error represented by the difference between its actual location and D_i. It is reasonable that this error may be distributed in a gaussian manner so that from Eq (50) the variance of that error is σ_D^2. Now σ_D can be determined as a function of x_1 and z_1 so that the result has a specified effect on $E(U_1)$. For example, if if x_1 = 1 m, $\lambda = 10.6\mu$, z_1 = 1 km, and σ_D = 1 mm, then $\exp\left(-\tfrac{1}{2}(\frac{2\pi x_1}{\lambda z_1})^2\sigma_D^2\right) = \exp(-0.18) = 0.84$. For a specified

amplitude reduction (for example 80% or about 1 db) and a given range z_1, the accuracy, σ_D, with which the laser positions must be made can be found. The result is

$$\sigma_D = \left(\frac{\lambda}{2\pi x_1}\right) z_1 \sqrt{2 \ln \eta} \tag{51}$$

where η is the specified reduction and σ_D, z_1, x_1, and λ are in meters. As z_1 increases, the necessary accuracy of the location of the elements decreases. A similar result could be derived for σ_d or a planar array with σ_D and σ_d.

As for Eq (37), the covariance of the field varies with element location as

$$\mathrm{Cov}(U_1, U_1') \propto \exp\left[-\left(\frac{2\pi x_1}{\lambda z_1}\right)^2 \sigma_D^2\right] \left(\exp\left[\left(\frac{2\pi x_1}{\lambda z_1}\right)^2 R_D(x-x')\right] - 1\right) \tag{52}$$

(Ref 26:159,476). But $R_D(x-x') = E(DD') = E(D)E(D') = D_i^2$ since D and D' are independent (i.e. the location of one element in no way influences the location of the next). Since the element locations are uncorrelated, $E(DD') = D_i^2 = \sigma_D^2$ and Eq (52) becomes

$$\mathrm{Cov}(U_1, U_1') \propto 1 - \exp\left[-\left(\frac{2\pi x_1}{\lambda z_1}\right)^2 \sigma_D^2\right] \tag{52a}$$

as in the temporal case (although Eq (38) is a variance and this is a covariance). Thus the results of Eq (49) indicate the complete time-space duality of this problem. The statistical results are similar for instabilities in time or space

(i.e. positional errors), and the general result contains all cases of interest.

The second physical positioning problem occurs when the optical axes of the lasers are not parallel. In this case Eq (14) becomes, for a linear array,

$$U_0(x,y,t) = \sum_i U_{0s}(x+D_i,y)\, A_i \exp\left[j\left(2\pi f_i t+\theta_i+\phi_i(t) + \frac{2\pi}{\lambda} x \sin o_i\right)\right] \qquad (53)$$

where o_i is the angle of the ith optic axis with respect to the normal to the array. For small angles, $\sin o_i \simeq o_i$ and the far field becomes

$$U_1(x_1,y_1,t) = U_1(x_1-2\pi z_1 o_i,y_1,t) \qquad (54)$$

where the frequency shifting property of Fourier transforms has been used (Ref 27:65). The angle o_i now affects two factors: $\exp\left[j\,\frac{\pi\tilde{q}}{\lambda z_1^2}(x_1-2\pi z_1 o_i)^2\right]$ from Eq (22) and $\exp\left[j\,\frac{2\pi D_i}{\lambda z_1}\,(x_1-2\pi z_1 o_i)\right]$ from Eq (42). For the coaxial case, the gaussian envelope behaves as in Eq (39), therefore using, for example, the Rayleigh criterion (Ref 15:354,360) the maximum o_i should be on the order of w_1 or about 3 mrad and no larger. Similar results are obtained for y in the two dimensional case.

One final, rather serious, problem in the area of laser position errors must be addressed. Eqs (26) and following were derived on the basis that all N beams that were superimposed propagated a distance z_1 into the far field. This

assumes that z_1 is measured from precisely the same point in each output beam (for example, the beam waist). If this is not true, i.e. if the waists are not perfectly aligned, then the z_1's are not the same and in fact must be represented as $z_1 + \Delta z_i$ where Δz_i is the offset of the ith beam. Substituting this new distance into Eq (26) indicates that Δz_i makes a negligible contribution everywhere except the $\exp(jk\Delta z_i)$ term in $P(x_1, y_1)$ (see Eq (18)). If $k\Delta z_i$ is folded into the interval 0 to 2π and is considered a gaussian random variable independent of $\phi_i(t)$, then $\exp(jk\Delta z_i) = \exp\left(-\frac{\sigma_z^2}{2}\right)$ where σ_z^2 is the variance of $k\Delta z_i$. Even if the beam waists could be perfectly aligned so that Δz_i was zero, vibrations, thermal expansion, and other effects would combine to create a Δz_i. Presumably this additional phase variation could be combined with $\phi_i(t)$ and compensated appropriately. However, even this requires that the optical path lengths from the point at which the beams are sampled to the detectors that form the first part of the phase locked loop must be equal. The bottom line is that for coherent combination, the relative phase of the lasers must be controlled precisely, and at optical wavelengths that is a very stringent requirement.

III. Coaxial Case

The coherent combination of several lasers coaxially, i.e. with the optical axes of the individual lasers coincident, led to a mean far field given by Eq (27). Certain simplifying assumptions produced Eq (31). This field is seen to be a temporal pulse train as an "envelope" on a "carrier" of frequency $f_0 - \left(\frac{N-1}{2}\right)\Delta f$ where f_0 is the original optical frequency. In addition, the signal has a peak amplitude of $AN\exp\left(-\frac{\sigma^2}{2}\right)$ and has a spatial distribution given by Eq (23) which describes a gaussian spherical wave. The temporal pulse train given by $\frac{\sin N\pi\Delta ft}{\sin \pi\Delta ft}$ whose characteristics are functions of N and Δf suggests that the signal could be used for ranging (as in a radar). If so, a measure is needed for the performance of such a system as a function of controllable parameters such as N and Δf.

Ambiguity Function

Before any performance criteria can be developed, there must be some assumptions regarding the receiver structure. Since this is not a receiver design study, only general assumptions will be made. (For further detail see Ref 6, 11, 23, 32, 37, and 40.) The first assumption of course is that the receiver employs coherent (heterodyne) detection (Ref 11:173-200). Aside from the requirement discussed in the previous section, this will result in better performance than in the direct detection case since

both amplitude and phase information are preserved. The heterodyne detector, however, is sensitive to spatial alignment, but this is not assumed to be a problem here. The second assumption is that a matched filter processor structure is used. For the case of signals in additive white gaussian noise (this is true in general for heterodyne receivers), the matched filter is the optimum receiver (Ref 6:18-32; 23:335-395; 40:311-317). The matched filter essentially correlates the received signal with a known signal and gives a peak response when the two signals are "matched." This of course requires that the receiver structure change if the signal changes. Fig. 5 is a representative system diagram. The third assumption is that certain physical phenomena that affect the optical signal as it is transmitted and reflected are ignored. These

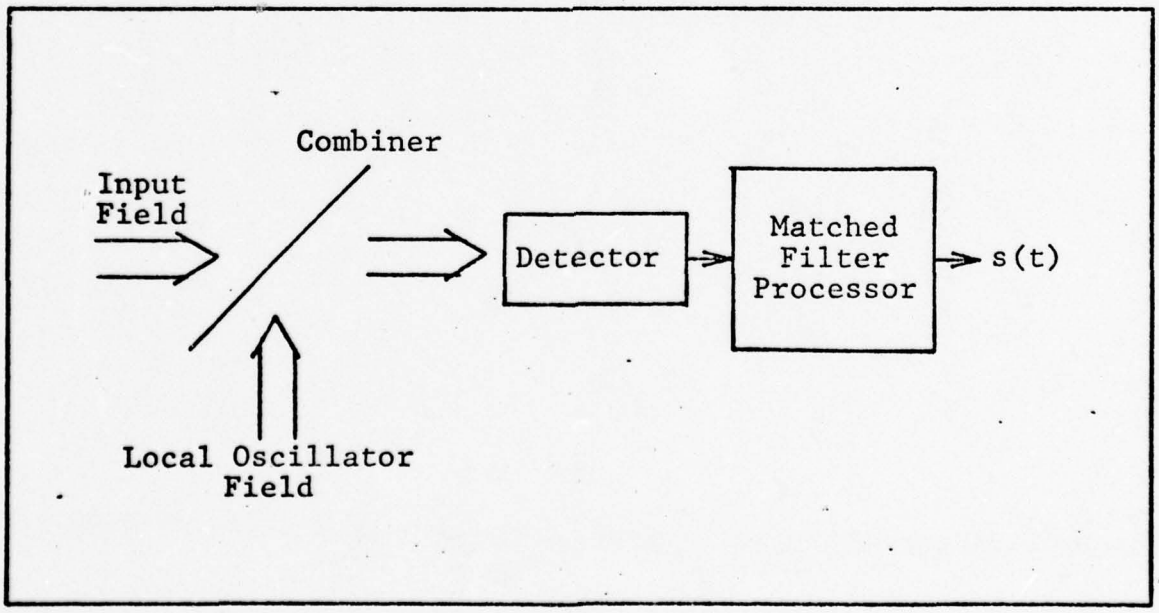

Fig. 5. System Diagram of Heterodyne Receiver

include such effects as path losses, field of view, losses in the optics, field alignment, aperture size, and others. These are ignored because they affect any signal in the same manner and therefore are unnecessary when comparing the relative performance of various signal structures.

Based on detection theory, the likelihood ratio is a function which, when compared to a threshold, produces an optimum decision of which signal was the "most likely" received. This likelihood function, in the case of a heterodyne receiver (and gaussian noise) with a matched filter processor, turns out to be proportional to

$$\chi(\tau,\nu) = \int_{-\infty}^{\infty} s(t)\, s^*(t-\tau) \exp\left(j2\pi\nu t\right) dt \qquad (55)$$

which is just a two dimensional correlation of a signal s(t) (which can be complex) with its time (τ) translated and doppler (ν) shifted version (Ref 6:59-108; 31:70-75,118-158; 37:275-313). The ambiguity function, $\chi(\tau,\nu)$, is a function of time delay, τ, that is related to the range of the target and doppler shift, ν, that is related to the velocity of the target. (χ is actually "normalized" so that $\chi(0,0)$ corresponds to some known τ_0 and ν_0.) The signal of interest here is just the mean of the far field in Eq (31). Since the only part of the signal envelope in Eq (31) that

varies with time is $\frac{\sin N\pi\Delta ft}{\sin \pi\Delta ft}$, and since the detector does the spatial integration of the field, the signal of interest will be considered to be

$$s(t) = A\exp\left(-\frac{\sigma^2}{2}\right) \frac{\sin N\pi\Delta ft}{\sin \pi\Delta ft} \tag{56}$$

where $A\exp\left(-\frac{\sigma^2}{2}\right)$ is retained explicitly as part of the amplitude of $s(t)$ and $\exp\left(-\frac{\sigma^2}{2}\right)$ is considered to be the strong signal approximation to the characteristic function of the partially controlled random phase, $\phi_i(t)$. Unfortunately, substituting Eq (56) into Eq (55) yields a result that is not immediately integrable to obtain $\chi(\tau,\nu)$. However, over a single period,

$$s(t) \approx \exp\left(-\frac{\sigma^2}{2}\right) \frac{\sin N\pi\Delta ft}{\pi\Delta ft} \tag{57}$$

This approximation gets better as N gets larger. Therefore,

$$\chi(\tau,\nu) = \frac{A^2}{\Delta f^2} \int_{-\infty}^{\infty} \frac{\sin N\pi\Delta ft}{\pi t} \frac{\sin N\pi\Delta f(t-\tau)}{\pi(t-\tau)} \exp(j2\pi\nu t)\,dt$$

$$= \frac{A^2}{\Delta f^2} \mathcal{F}_t\{s(t)\ s(t-\tau)\}$$

$$= \frac{A^2}{\Delta f^2} \mathcal{F}_t\{s(t)\} * \mathcal{F}_t\{s(t-\tau)\}$$

$$= \frac{A^2}{\Delta f^2} \mathcal{F}_t\{s(t)\} * \exp(j2\pi\nu\tau)\mathcal{F}_t\{s(t)\} \tag{58}$$

Now, by the duality property of ambiguity functions (Ref 37:309-310)

$$\chi(\tau,\nu) = \chi_1(\nu,-\tau)$$

where χ is the ambiguity function of s(t) whose Fourier transform is $S_1(f)$ (whose ambiguity function is $\chi_1(\tau,\nu)$). Now the Fourier transform of s(t) in Eq (58) is just a square pulse of height 1 and width $N\Delta f$ whose ambiguity function is given by (Ref 37:280)

$$|\chi_1(\tau,\nu)| = \begin{cases} \left(1 - \frac{|\tau|}{N\Delta f}\right)\left|\frac{\sin N\pi\Delta f\nu\left(1 - \frac{|\tau|}{N\Delta f}\right)}{\pi\nu\left(1 - \frac{|\tau|}{N\Delta f}\right)}\right|, & |\tau| \le N\Delta f \\ 0, \text{ elsewhere} \end{cases} \tag{59}$$

Therefore,

$$|\chi(\tau,\nu)| = \frac{A^2}{\Delta f^2}|\chi_1(\nu,-\tau)|$$

$$= \frac{A^2}{\Delta f^2}\left(1 - \frac{|\nu|}{N\Delta f}\right)\left|\frac{\sin \pi N\Delta f(-\tau)\left(1 - \frac{|\nu|}{N\Delta f}\right)}{\pi(-\tau)\left(1 - \frac{|\nu|}{N\Delta f}\right)}\right|$$

$$= \begin{cases} \frac{A^2}{\Delta f^2}\left(1 - \frac{|\nu|}{N\Delta f}\right)\left|\frac{\sin N\pi\Delta f\tau\left(1 - \frac{|\nu|}{N\Delta f}\right)}{\pi\tau\left(1 - \frac{|\nu|}{N\Delta f}\right)}\right|, & |\nu| \le N\Delta f \\ 0, \text{ elsewhere} \end{cases} \tag{60}$$

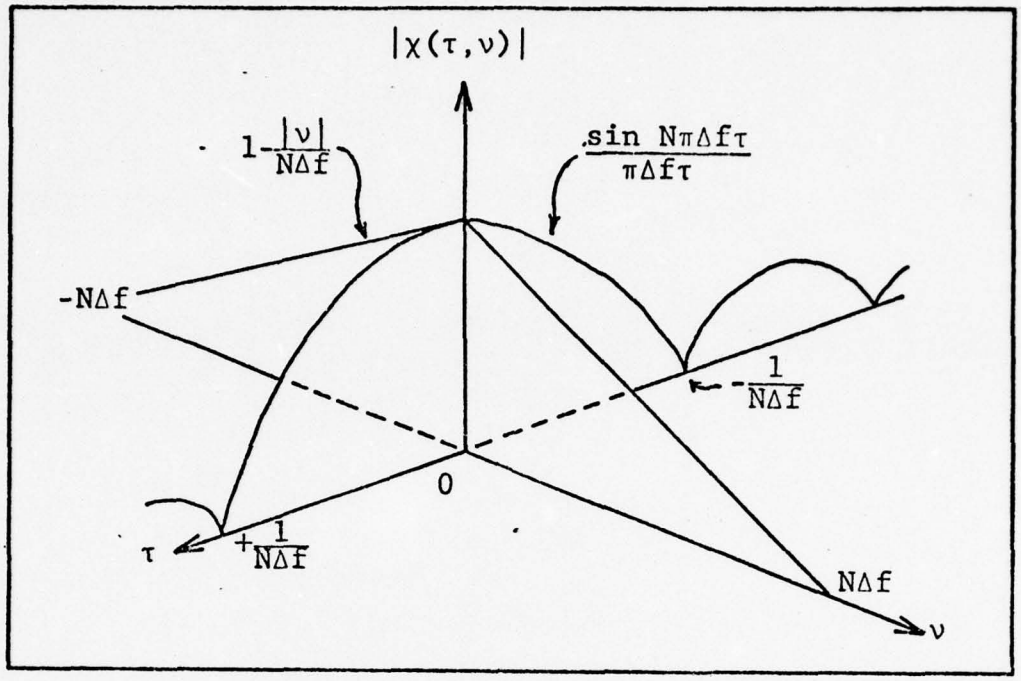

Fig. 6. Ambiguity Function of $\sin(N\pi\Delta ft)/\pi\Delta ft$

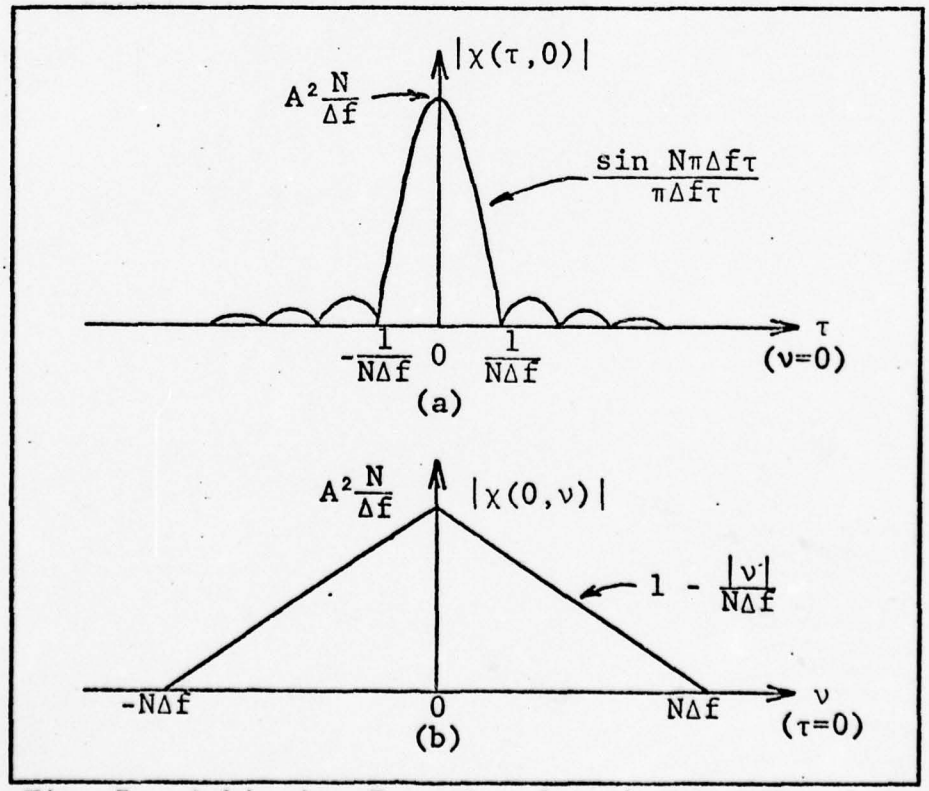

Fig. 7. Ambiguity Function for a) Known Doppler and b) Known Delay

Eq (60) is sketched in Fig. 6 on Page 43. $|\chi(\tau,0)|$ is shown in Fig. 7a, and $|\chi(0,\nu)|$ is shown in Fig. 7b found on Page 43.

It is now possible to obtain Cramer-Rao lower bounds for estimates of τ and ν in terms of the signal energy to noise ratio, the bandwidth of the signal, and the duration of the signal. These are estimates of delay time and doppler velocity for a given signal structure that has an ambiguity function $\chi(\tau,\nu)$. The (parameter) estimate of delay is denoted $\hat{\tau}$ and that of doppler is denoted $\hat{\nu}$. The variances (and standard deviations) of these estimates are a measure of the precision of the measurement, i.e a smaller variance implies a more precise measurement. Following Ref 31:70-74 and 37:294-299 the results are

$$\sigma_\tau = \left(\mathrm{Var}(\hat{\tau}-\tau)\right)^{\frac{1}{2}} \geq \left(\sqrt{\frac{2E}{N_0}}\,\gamma\right)^{-1} \tag{61}$$

$$\sigma_\nu = \left(\mathrm{Var}(\hat{\nu}-\nu)\right)^{\frac{1}{2}} \geq \left(\sqrt{\frac{2E}{N_0}}\,\delta\right)^{-1} \tag{62}$$

where σ_τ is the standard deviation of the delay estimator $\hat{\tau}$, σ_ν is the standard deviation of the doppler estimator $\hat{\nu}$, the signal energy is assumed to be much larger than the noise, the noise is given by the height, $\frac{N_0}{2}$, of its power spectral density (the noise is assumed to be white and gaussian), and γ and δ are

$$\gamma^2 = 4\pi^2 \int_{-\infty}^{\infty} f^2 |S(f)|^2 df \tag{63}$$

$$\delta^2 = 4\pi^2 \int_{-\infty}^{\infty} t^2 |s(t)|^2 dt \tag{64}$$

where γ represents the rms bandwidth of the signal s(t) and δ represents the rms duration of the signal. (Eqs (63) and (64) were derived in Ref 31 and 37 for normalized signals s(t) and S(f).) Eqs (61) and (62) also assume that there is no coupling between γ and δ, i.e. that there is no linear frequency modulation component (Ref 31:74). Now, the range precision and range rate precision respectively are given by (Ref 31:74)

$$\sigma_R = \frac{c}{2} \sigma_\tau \tag{65}$$

$$\sigma_{\dot{R}} = \frac{\lambda}{2} \sigma_\nu \tag{66}$$

The signal energy, E, is found from Eq (56) in series form,

$$|s(t)| = \exp\left(-\frac{\sigma^2}{2}\right)\left|\frac{\sin N\pi\Delta ft}{\sin \pi\Delta ft}\right|$$

$$= \exp\left(-\frac{\sigma^2}{2}\right)\sum_i (\exp(j2\pi\Delta ft))^i$$

Therefore,

$$E = \int_{T_p} |s(t)|^2 dt$$

where $T_p = \frac{1}{\Delta f}$ is a period (Eq (33)) so that

$$E = \int_{-\frac{1}{2\Delta f}}^{\frac{1}{2\Delta f}} \left(A\exp\left(-\frac{\sigma^2}{2}\right) \sum_i \left(\exp(j2\pi\Delta f t)\right)^i \right)^2 dt$$

$$= A^2\exp\left(-\sigma^2\right) \int_{-\frac{1}{2\Delta f}}^{\frac{1}{2\Delta f}} \left(N + \sum_{i\neq k}\sum \exp\left(j2\pi(i-k)\Delta f t\right) \right) dt$$

$$= A^2\exp\left(-\sigma^2\right) \left(\frac{N}{\Delta f} + \sum_{i\neq k}\sum \frac{\sin \pi(i-k)}{\pi(i-k)\Delta f} \right)$$

$$= A^2\exp\left(-\sigma^2\right) \frac{N}{\Delta f} \qquad (67)$$

Eq (60) was derived from the approximation in Eq (57). This approximation is good only for a single period of the signal, s(t) (Eq (56)). However, s(t) is periodic in t and can be represented as

$$s(t) = \sum_{i=0}^{m-1} s_a(t - iT_p)$$

$$= \sum_i s_a\left(t - \frac{i}{\Delta f}\right)$$

where m is the number of repetitions of $s_a(t)$, $s_a(t)$ is the approximation over a single period T_p, and $T_p = \frac{1}{\Delta f}$. Now the ambiguity function of s(t) becomes

$$\chi(\tau,\nu) = \sum_{p=-(m-1)}^{m-1} \exp\left(j\pi\nu(m-1+p)\frac{1}{\Delta f}\right) \chi_a\left(\tau - \frac{p}{\Delta f}, \nu\right) \left(\frac{\sin \pi\nu(m-|p|)\frac{1}{\Delta f}}{\sin \pi\nu\frac{1}{\Delta f}} \right)$$

where $\chi_a(\tau,\nu)$ is given by Eq (60) (Ref 31:185-186). It is

seen that the new ambiguity function is just the sum of the old ambiguity functions shifted on the delay axis by intervals of $\frac{1}{\Delta f}$ and multiplied by a weighting term. The magnitude of the pth term of the ambiguity function is just (Ref 31:187),

$$|\chi(\tau,\nu)|_{\text{at } p} = \left|\chi_a\left(\tau-\frac{p}{\Delta f},\nu\right)\right|\left|\frac{\sin \pi\nu(m-|p|)\frac{1}{\Delta f}}{\sin \pi\nu\frac{1}{\Delta f}}\right| \qquad (68)$$

Thus there are delay ambiguities at intervals of $\frac{1}{\Delta f}$ and a fine structure (due to $\frac{\sin \pi\nu(m-|p|)\frac{1}{\Delta f}}{\sin \pi\nu\frac{1}{\Delta f}}$) in doppler with intervals of Δf. Now some specific applications for a coaxial system whose far field is given by Eq (31) can be considered.

Range Measurement

When only range measurements are desired, the doppler is considered to be known, i.e. tracked (or zero for a stationary target). If the doppler is unknown, then it must be considered at the same time τ is considered i.e. jointly estimated (this is done later in this section), or the ambiguity function must be broad along the ν axis so that there is little chance of error in estimating τ. Therefore the interest in $\chi(\tau,\nu)$ is just along the τ axis. Fig. 7a is the τ axis for a single pulse. Multiple pulses (Eq (68)) would produce a periodic function with amplitude weighting. As long as the round trip time (delay) of a

pulse is less than the pulse rate, there is no ambiguity as to which peak on the τ axis is involved. The width of the central peak in Fig. 7a is a crude measure of the precision with which the target range can be measured. Basically, this precision is a function of $\frac{1}{N\Delta f}$ so that as the total spectral width of the field is increased the range precision can be made arbitrarily good within the limit that $N\Delta f$ is less than or equal to the gain line width of the lasers. Explicitly, the range precision is found by combining Eqs (61) and (65) to obtain

$$\sigma_R \geq \frac{c}{2\sqrt{\frac{2E}{N_0}}\,\gamma} \tag{69}$$

Now from Eq (63),

$$\gamma^2 = 4\pi^2 \int_{-\infty}^{\infty} f^2 |S(f)|^2 df$$

if S(f) is normalized. If S(f) is not normalized then

$$\gamma^2 = 4\pi^2 \frac{\int_{-\infty}^{\infty} f^2 |S(f)|^2 df}{\int_{-\infty}^{\infty} |S(f)|^2} \tag{70}$$

Now, from Eq (57)

$$s(t) = A\exp\left(-\frac{\sigma^2}{2}\right)\frac{\sin N\pi\Delta f t}{\pi\Delta f t}$$

Therefore,

$$S(f) = \begin{cases} A\exp\left(-\frac{\sigma^2}{2}\right)\frac{1}{\Delta f}, & |f| \le \frac{N\Delta f}{2} \\ 0, \text{ elsewhere} \end{cases}$$

$$\gamma^2 = 4\pi^2 \frac{2\int_0^{\frac{N\Delta f}{2}} f^2 \left(\frac{1}{\Delta f}\right)^2 df}{2\int_0^{\frac{N\Delta f}{2}} \left(\frac{1}{\Delta f}\right)^2 df}$$

$$= \frac{\pi^2}{3} N^2 \Delta f^2 \qquad (71)$$

So that using Eqs (67) and (71) in (69),

$$\sigma_R \ge \frac{c}{2\sqrt{\frac{2A^2\exp\left[-\sigma^2\right]N}{N_0\Delta f}\left(\frac{\pi^2}{3}(N\Delta f)^2\right)}}$$

$$\ge \frac{c\sqrt{3N_0}}{\sqrt{8\pi^2A^2\exp\left[-\sigma^2\right]N^3\Delta f}} \qquad (72)$$

Eq (72) shows that the range measurement precision is proportional to $\frac{1}{N\sqrt{N\Delta f}}$ which is in line with what was expected. Since $N\Delta f$ is the total bandwidth of the signal without regard to the frequency spacings, the assumption of $f_i = i\Delta f$ was not really restrictive. Eq (72) then is a rather general result that represents the best possible range measurement precision obtainable by the temporal signal in the mean far field of Eq (27).

Velocity Measurement

In the dual case, a similar derivation can be made for doppler (velocity) measurement precision. In this case the

range is presumed known (or the ambiguity function is broad in τ), so that the interest in $\chi(\tau,\nu)$ is only along the ν axis. Fig. 7b is the ν axis for a single pulse. Multiple pulses introduce a fine structure as given in Eq (68). For a single pulse, the crude doppler measurement precision improves as $N\Delta f$ gets small. This implies that increasing $t_p = \frac{2}{N\Delta f}$ also increases the doppler precision. Basically, this says that the more information that is received (i.e. the longer the pulse), the better the doppler precision can be made. From Eqs (62) and (66)

$$\sigma_{\dot{R}} \geq \frac{\lambda}{2\sqrt{\frac{2E}{N_0}}\,\delta} \tag{73}$$

and from Eq (64),

$$\delta^2 = 4\pi^2 \int_{-\infty}^{\infty} t^2 |s(t)|^2 dt$$

so that for the unnormalized $s(t)$ of Eq (57)

$$\delta^2 = 4\pi^2 \frac{\int_{-\infty}^{\infty} t^2 |s(t)|^2 dt}{\int_{-\infty}^{\infty} |s(t)|^2 dt} \tag{74}$$

Therefore for a single pulse, $\int_{-\infty}^{\infty} |s(t)|^2 dt = A^2 \exp(-\sigma^2) \frac{N}{\Delta f}$ as in Eq (67) and

$$\int_{-\infty}^{\infty} t^2 |s(t)|^2 dt = \frac{A^2 \exp(-\sigma^2)}{\pi^2 \Delta f^2}\, 2 \int_0^{\frac{1}{2\Delta f}} \sin^2 N\pi\Delta f t \; dt$$

$$= \frac{A^2 \exp(-\sigma^2)}{\pi^2 \Delta f^2} \left(\frac{1}{2\Delta f}\right) \tag{75}$$

where the integral has been taken over a single period of the signal. For m pulses, the signal energy is multiplied by m so that Eq (74) becomes

$$\delta^2 = 4\pi^2 \frac{A^2 \exp(-\sigma^2)}{\pi^2 \Delta f^2} \left(\frac{m}{2\Delta f}\right) \left[\frac{mA^2 \exp(-\sigma^2) N}{\Delta f}\right]^{-1}$$

$$= \frac{2}{N\Delta f^2} \tag{76}$$

and δ is seen to be independent of the number of pulses notwithstanding the fine structure on the doppler axis given in Eq (68). This just indicates that the doppler precision is affected only by the pulse width and not the number of pulses. The fine structure in Eq (68) tends to improve the resolution of targets with similar doppler velocities, but it also increases the number of doppler ambiguities (peaks) (Ref 31:191). Eq (76), however, is concerned only with measurement precision and not resolution, i.e. local accuracy without regard to ambiguity. Now using Eqs (67) and (76) in (73),

$$\sigma_{\dot{R}} \geq \frac{\lambda}{2\sqrt{\frac{2A^2 \exp(-\sigma^2) N\ 2}{N_0 \Delta f\ N\Delta f^2}}}$$

$$\geq \frac{\lambda \sqrt{N_0 \Delta f^3}}{\sqrt{16\ A^2 \exp(-\sigma^2)}} \tag{77}$$

and the doppler precision depends only on Δf.

This result is slightly different from what was expected from inspection of Eq (60) since N does not appear

in Eq (77). The reason is found in Eq (75) where the rms signal duration was determined for a period. When this is done for square temporal pulses (as in radar theory), the result is an integral over the pulse width. If this is done here, by analogy, then Eq (76) becomes

$$\delta^2 = \frac{2}{N^2 \Delta f^2} \tag{76a}$$

so that Eq (77) becomes

$$\sigma_{\dot{R}} \geq \frac{\lambda \sqrt{N_0 N \Delta f^3}}{\sqrt{16\ A^2 \exp\left(-\sigma^2\right)}} \tag{77a}$$

The discrepancy occurs because s(t) is of infinite duration. This is the dual of the radar problem where the ideal rectangular signals have infinite mean square bandwidth (Ref 31:49-50). In that case the signal is considered band limited and appropriate approximations made. The result is dependent on rms pulse width as it is in Eq (77a) for this case. However, for the lasers, even though the signal is, strictly speaking, time limited (it is at least causal) the infinite result may be more closely approximated here than for the radar case. Thus Eqs (77) and (77a) represent an interesting dichotomy of results that are both reasonable, but both different. These equations represent the best possible precision in doppler measurement (when range is known) that can be obtained from the field of Eq (31).

Coupled Measurements

It is often desirable to make measurements of both range and velocity, i.e. the case where both are unknown. Eqs (72) and (77) or (77a) are still valid as long as there is no linear frequency modulation on the signal, i.e. the complex envelope is real (Ref 31:74; 37:299). If this is the case, the range precision can be improved by increasing N or Δf. However, increasing Δf degrades doppler precision relatively rapidly. By increasing N, it is possible to improve range precision while the doppler precision remains the same (Eq (77)) or degrades more slowly (Eq (77a)). Doppler precision can be increased by decreasing Δf, but to maintain the range precision, N must be increased accordingly. This is a rather nice result although increasing N becomes prohibitively expensive at some point (even for the Federal Government) so there is a limit on the range and doppler precision that can be obtained. In addition, since $N\Delta f$ must be at most equal to the laser gain line width, as N is increased, Δf is decreased. This coupling between N and Δf further complicates the task of obtaining the best possible simultaneous range and velocity precisions.

It is possible to improve σ_R and $\sigma_{\dot{R}}$ simultaneously by increasing the energy to noise ratio, $\frac{E}{N_0}$. If N_0 is fixed, this can be accomplished by increasing E. From Eq (67), E can be increased by increasing N or decreasing Δf with the same effects on σ_R and $\sigma_{\dot{R}}$ noted above. E can also be increased by decreasing the variance of the phase, i.e.

controlling the phase more tightly, or by increasing A. Both of these approaches can be taken, but both have limits; for example, σ can be made no smaller than zero, and A is limited by the size of the laser gain medium as well as other characteristics of the laser.

The simplest way to increase E without changing N_0, N, or Δf is just to collect more pulses. Eq (67) was developed for the energy of a single period, $T_p = \frac{1}{\Delta f}$. If m pulses are used, the energy in Eq (67) increases linearly with m, and σ_R and $\sigma_{\dot{R}}$ from Eqs (72) and (77) are improved accordingly. This approach is only limited by the number of pulses that can be received and by the assumption that the target range and doppler are not changing appreciably during the observation period (Ref 31:70).

One additional case of interest is that of introducing some sort of frequency or phase modulation on the signal s(t). This could be implemented, conceptually at least, by modulating all of the lasers simultaneously and in the same manner. A simple case is that of linear frequency modulation where

$$s_m(t) = s(t)\exp\left(j\pi g t^2\right) \tag{78}$$

By a property of ambiguity functions (Ref 31:123; 37:290)

$$\chi_m(\tau,\nu) = \chi(\tau,\nu-g\tau)$$

$$|\chi_m(\tau,\nu)| = \begin{cases} A\,\frac{N}{\Delta f}\left(1-\frac{|\nu-g\tau|}{N\Delta f}\right)\left|\frac{\sin N\pi\Delta ft\left(1-\frac{|\nu-g\tau|}{N\Delta f}\right)}{N\pi\Delta ft\left(1-\frac{|\nu-g\tau|}{N\Delta f}\right)}\right|, & |\nu-g\tau| \leq N\Delta f \\ 0, \text{ elsewhere} \end{cases} \tag{79}$$

This transformation, in effect, shears the old ν axis to $\nu = g\tau$. This will decrease the size of the central peaks on the τ and ν axes so that if either range or doppler is known, the other may be determined with better precision than before. However, for the coupled case, the Cramer-Rao lower bounds are increased as shown in Ref 31:73-74 and 37:298. Hence a simple linear modulation is not helpful to the coupled measurement case. Much more complex modulations such as pulse coding (Ref 37:314-323) may be more useful, but their implementation for N lasers would probably be very difficult.

IV. Linear Array

The mean far field for a planar array of lasers was given by Eq (44). This equation cannot be reduced to a convenient closed form for the general case. It can be solved numerically for a given set of A_{ik}, f_{ik}, θ_{ik}, and σ_{ik}, but some simplifying assumptions are needed before any further analysis is possible. The first such assumption that will be used throughout this section is that the array will be considered one dimensional, i.e. a linear array. Most of the results can be extended to two or more dimensions if desired, and, in fact, one special case of a planar array will be considered. Nevertheless, the important results can be demonstrated with a linear array. The second assumption used in this section is that the locations of the lasers are precisely known. Therefore, Eq (50) can be rewritten for $\sigma_D = 0$ as,

$$E\left(U_1(x_1,y_1,t)\right) = P(x_1,y_1)U_{1s}(x_1,y_1)\exp\left(-\frac{\sigma^2}{2}\right)\sum_i A_i\exp\left(j\left(2\pi f_i t + \frac{2\pi D_i x_1}{\lambda z_1} + \theta_i\right)\right) \quad (80)$$

Because of the $\frac{2\pi D_i x_1}{\lambda z_1}$ term in the exponent, this mean field has a spatial modulation within the overall gaussian envelope described by $P(x_1,y_1)U_{1s}(x_1,y_1)$. The performance measures in this section will deal with the characteristics of this spatial modulation in terms of N, f_i, D_i, and θ_i and, for certain applications, will consider peak-to-side lobe ratios.

Pattern Characteristics

In order to maintain the pulsed nature of the signal used in the coaxial case, the first assumption used here is that $f_i = i\Delta f$; other cases will be discussed later. In addition, θ_i is a simple phase shift that merely determines an absolute reference for either the time or space coordinates. Hence, with no loss in generality, it can be assumed to be zero. An interesting use for θ_i will be discussed later.

Scanning. For uniform aperture excitations ($A_i = A$) and considering a uniform array where $D_i = iD$, Eq (80) becomes

$$E\left[U_1(x_1,y_1,t)\right] = P(x_1,y_1)U_{1S}(x_1,y_1)A\exp\left[-\frac{\sigma^2}{2} + j\left(\frac{N-1}{2}\right)\right.$$

$$\left.(2\pi\Delta ft+\frac{2\pi Dx_1}{\lambda z_1})\right]\frac{\sin N\pi\left[\Delta ft + \frac{Dx_1}{\lambda z_1}\right]}{\sin \pi\left[\Delta ft + \frac{Dx_1}{\lambda z_1}\right]} \qquad (81)$$

As before, the exponential factor indicates a shift of the optical frequency to $f_o-\left(\frac{N-1}{2}\right)\Delta f$, but it also indicates that there is now a spatial frequency because of the $\frac{2\pi Dx_1}{\lambda z_1}$ term. The ratio of sinusoids in Eq (81) can be written as a function of $\frac{N}{2}(k'x_1+\omega t)$ where $k' = \frac{D}{z_1}\left(\frac{2\pi}{\lambda}\right)$ and $\omega=2\pi\Delta f$. This is the standard form of a classical travelling wave whose profile is given at $t = 0$, temporal period is $\frac{2\pi}{\omega}$, phase velocity is $\frac{\omega}{k'}$, and spatial period is $\frac{2\pi}{k'}$. Therefore,

$$\left.\begin{aligned}
\text{Temporal period} &= T_p = \frac{2\pi}{\omega} = \frac{1}{\Delta f} \text{ sec (Eq (33))} \\
\text{Temporal pulse width} &= t_p = \frac{2}{N\Delta f} \text{ sec (Eq (32))} \\
\text{Phase velocity} &= \frac{\omega}{k} = \frac{\Delta f \lambda z_1}{D} \frac{m}{sec} \\
\text{Spatial period} &= X_p = \frac{2\pi}{k} = \frac{\lambda z_1}{D} \text{ m} \\
\text{Spatial pulse width} &= x_p = \frac{2\lambda z_1}{ND} \text{ m}
\end{aligned}\right\} \quad (82)$$

The spatial beam profile at t = 0 is identical (within a scaling constant) to the temporal profile at $x_1 = 0$ as shown in Fig. 4. Therefore, in addition to the temporal pulse train, there is now a spatial pulse train scanning linearly in x_1 at a rate of $\frac{1}{T_p} = \Delta f$ Hz. This still occurs beneath the gaussian envelope. From Eq (39), for $\lambda = 10.6\mu$, $z_1 = 1$ km, and w = 1 mm, the waist at z_1 is about 3.5 m. The beam width is equivalent to x_p which for an array dimension ND = 1 m is about 2 cm. For D = 1 cm (this would be for an array of 100 lasers spaced 1 cm apart), the spatial period is about 1 m. The result is illustrated in Fig. 8. The small beams measured by x_p will move right or left (depending on whether $f_i = i\Delta f$ or $(N - i)\Delta f$, i.e. whether the frequency offsets step "up" the array or "down" the array) at a speed of $\frac{\Delta f \lambda z_1}{D} \frac{m}{sec}$ and the pattern will repeat every $\frac{1}{\Delta f}$ sec. Unfortunately, x_p places more stringent restrictions on the misalignment angles of the laser optical

axes as shown by Eq (54). Now the maximum o_i should be on the order of $\frac{x_p}{2}$ or about 10^{-5} rad. This is two orders of magnitude more restrictive than the 10^{-3} rad for the coaxial case.

This is a useful result for a system that does not require resolution of close targets in azimuth to less than about w_1 and does require multiple target returns (for example to reduce glint or other transient phenomena). Unfortunately, it also complicates the ambiguity problem as there is no way to distinguish which beam, x_p, is providing the return. Therefore, the resolution capability inherent in the small x_p is being wasted. These side lobes away from the $x_1 = 0$ peak are called "grating lobes"

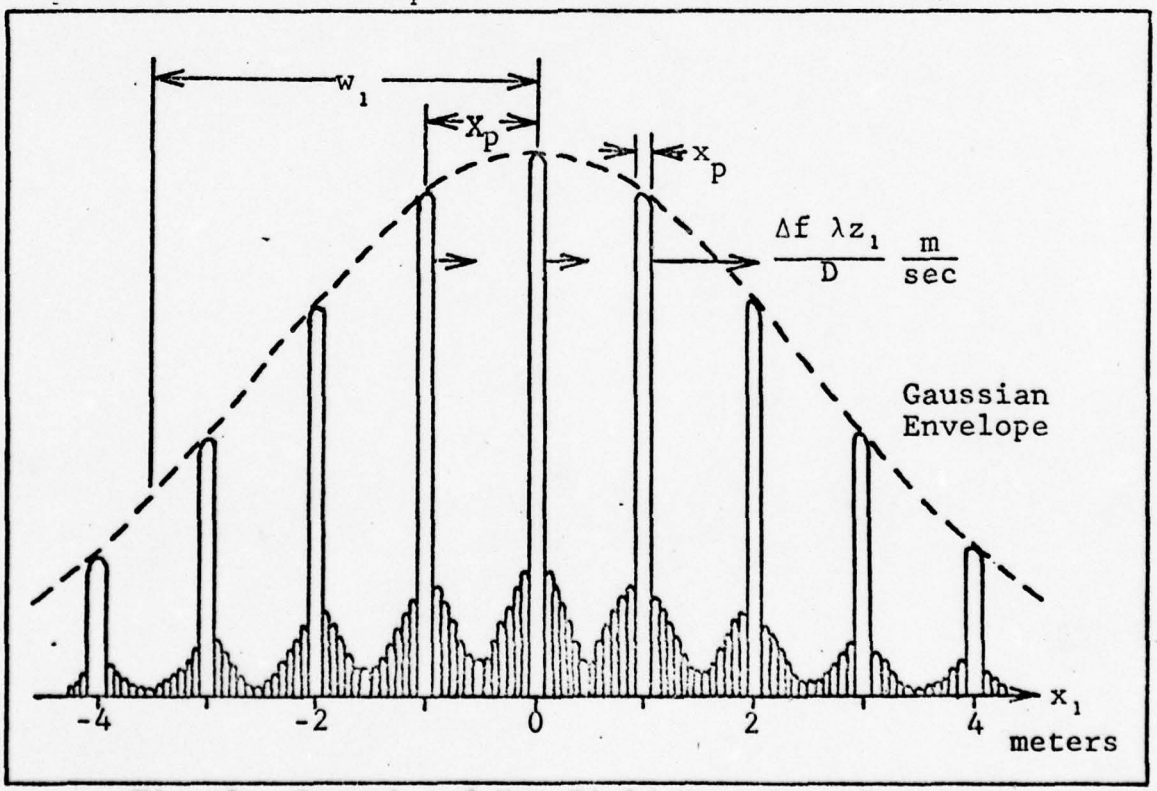

Fig. 8. Example of Far Field Mean Beam Pattern for N=100, D=1 cm, z_1=1 km.

in radar theory. It can be shown that these lobes do not exist if $D<\frac{\lambda}{2}$ (Ref 35:90) which is impossible at optical wavelengths. Eqs (39) and (82) suggest two possible solutions. If the waist, w_1, could be made sufficiently small ($<X_p$) then the gaussian envelope could be made to attenuate unwanted lobes. From Eq (39) the only way to do this is to increase w. For significant attenuation of the first side lobes, $w_1 \leq \frac{X_p}{2}$, therefore $w \geq \frac{2D}{\pi}$. This is not desirable since originally the laser aperture radius was chosen to be $\frac{3w}{2}$ to minimize diffraction effects and maximize power transmission. Hence the aperture radius must be at least on the order of the aperture separation, and the apertures overlap. Eq (82) indicates that X_p can be increased by decreasing D and similar results are obtained, i.e. the apertures overlap. Thus for $D>\frac{\lambda}{2}$, there is only one other way to eliminate the grating lobes and that is to use an aperiodic array, i.e. $D_i \neq iD$. This case will be discussed at the end of this section.

Pattern Shape. So far the amplitudes, A_i, of the lasers have been assumed to be equal and the result has been a $\frac{\sin Nx}{\sin x}$ pattern in space, Eq (81). It is useful to pursue a slightly different analysis of Eq (80) for two reasons: 1) more flexibility may be obtained if the A_i are not all the same, and 2) the side lobe structure of Eq (81) may not be desirable. In Eq (81), the first side lobe is the highest. Fig. 9 shows the peak-to-first-side lobe ratio as a function of N. Therefore, even as the number

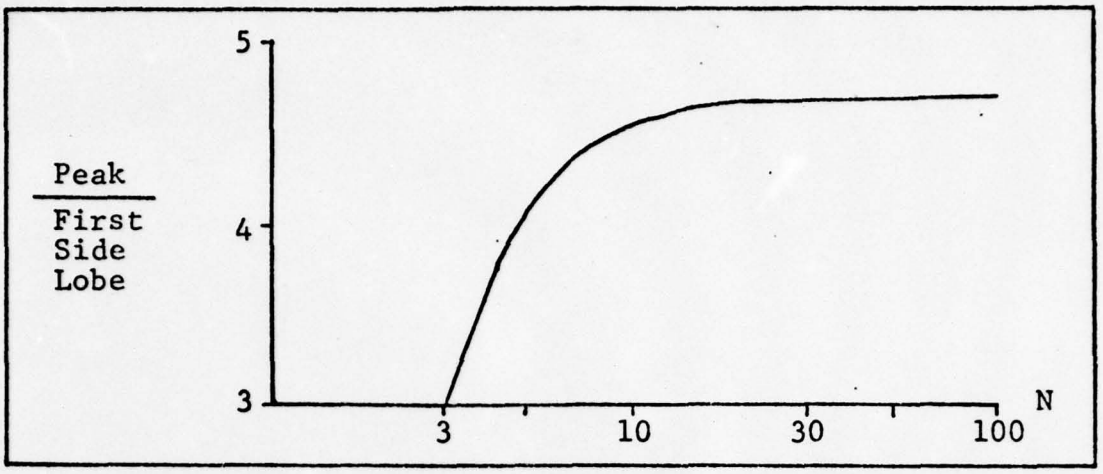

Fig. 9. Peak-to-First-Side Lobe Ratio versus N for sin(Nx)/sin(x).

of lasers increases, after N ≈ 20 the highest side lobe grows linearly with the peak.

If Eq (80) is rewritten for $f_i = i\Delta f$, $D_i = iD$, and $\theta_i = i\theta$ the result is

$$E\left[U_1(x_1,y_1,t)\right] = P(x_1,y_1)U_{1s}(x_1,y_1)\exp\left(-\frac{\sigma^2}{2}\right)\sum_i A_i z^i \quad (83)$$

where

$$z = \exp\left[j\left(2\pi\Delta f t + \frac{2\pi D x_1}{\lambda z_1} + \theta\right)\right] \quad (84)$$

and the series in Eq (83) can be written

$$\sum_i A_i z^i = A_{N-1}\prod_i (z-z_i) \quad (85)$$

which is just a polynomial in z (Ref 35:87). Eq (84) is referred to in antenna theory as a z transform. (For a more general discussion of antenna theory, see, for example, Ref 5; properties of z transforms and their uses may be found in Ref 25:45-77 and 35:87-111.) Now, Eq (84) can be written

$$z = \exp\left[j\left(\frac{2\pi}{\lambda}\right)D\left(\frac{x_1}{z_1} + \left\{\frac{\lambda\Delta ft}{D} + \frac{\lambda\theta}{2\pi D}\right\}\right)\right]$$

$$= \exp\left[j\left(\frac{2\pi}{\lambda}\right)D\left(\frac{x_1}{z_1} - \sin\theta_0\right)\right] \qquad (86)$$

where $\frac{x_1}{z_1}$ in the far field approximation is the angle of observation with respect to the z axis (optical axis) and θ_0 represents the angle at which the "main lobe" is pointing (Ref 35:89) as shown in Fig. 10.

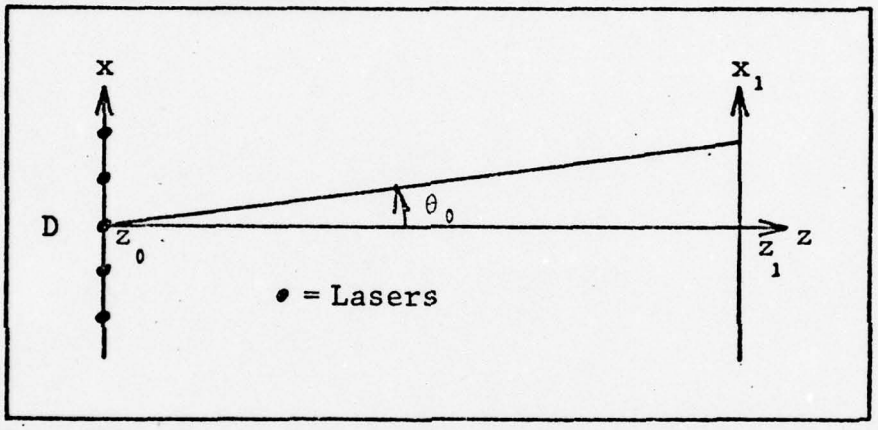

Fig. 10. Geometry of Linear Array and Far Field

Of course, $|\sin\theta_0|$ cannot be greater than 1 so that values of $\left(\frac{\lambda\Delta ft}{D} + \frac{\lambda\theta}{2\pi D}\right)$ that are greater than 1 essentially represent beam angles outside of the "visible" region. In fact, $\left(\frac{\lambda\Delta ft}{D} + \frac{\lambda\theta}{2\pi D}\right)$ may be considered modulo 2π, i.e. $\left(\frac{\lambda\Delta ft}{D} + \frac{\lambda\theta}{2\pi D}\right) = 2n\pi + \sin\theta_0$ where $n = 0, \pm1, \pm2, \ldots$ and $|\sin\theta_0| \leq 1$ (Ref 35:89). Therefore, in Eq (86) the main beam location is a function of time as was shown by Eq (82). It is now possible to choose the zeroes and amplitude weightings of the polynomial in Eq (85) to yield desirable beam width or side lobe properties (see, for example, Ref 30, 36, and

Ref 35:95-110). The array can, in fact, be designed so that the side lobes are always below a given design value (which can be made much lower than the results in Fig. 9) for a given main beam width (this is called a Chebyshev array; Ref 35:111-118). Thus, with this approach the side lobes may be better controlled, however, there are still grating lobes because $D>\frac{\lambda}{2}$.

It is interesting to note that by duality similar results can be obtained for the temporal pulse train represented by Eq (31). In this case, for $x_1 = 0$, the zeroes of Eq (85) may be chosen so that the temporal side lobes are controlled in a desired manner. Presumably appropriate z_i and A_i could be chosen to control the temporal and spatial side lobes simultaneously.

Monochromatic Beam

The z transforms also indicate another interesting possibility. If in Eq (86), $\Delta f = 0$, then the beam position is not a function of time; it is only a function of θ. This represents the case of a continuous wave resultant beam where all N lasers are oscillating at the same frequency, f_0, and are being added coherently with a controllable phase offset, θ, across the array. This case is very similar to the phased array in antenna theory.

Beam Steering. For $\Delta f = 0$, Eq (86) becomes

$$z = \exp\left[j\left(\frac{2\pi}{\lambda}\right)D\left(\frac{x_1}{z_1} - \theta_0\right)\right] \tag{87}$$

where $-\theta_0 \approx \frac{\lambda\theta}{2\pi D}$ since θ_0 is small. For the linear array, then, the main beam may be pointed anywhere within the gaussian envelope by proper choice of θ. (Of course, because of the grating lobes, one "main beam" is indistinguishable from its neighbor and in fact all of the lobes move simultaneously with θ. Nevertheless a "main beam" is referred to for convenience.) If desired, the main beam may be made to scan sinusoidally for

$$-\theta_0 = \frac{\lambda\theta}{2\pi D}$$

$$= r\sin 2\pi f_s t$$

$$\theta = \frac{2\pi D r}{\lambda} \sin 2\pi f_s t \qquad (88)$$

where r is a scale factor that determines the limits of the scan displacement and f_s is the sinusoidal scan rate. Two such arrays arranged orthogonally would provide two sets of pencil beams that scan orthogonally. Such a system could be used for tracking a target.

Planar Array. For the special case of $f_i = \Delta f = 0$, $A_{ik} = A$, $\sigma_{ik} = \sigma$, $D_{ik} = D$, and $d_{ik} = d$, Eq (44) may be written as

$$E\left[U_1(x_1,y_1,t)\right] = P(x_1,y_1)U_{1s}(x_1,y_1)A\exp\left[-\frac{\sigma^2}{2}\right]\Sigma\Sigma_{ik}$$
$$\exp\left[j\left(\frac{2\pi}{\lambda}\right)\left(D\frac{x_1}{z_1}+d\frac{y_1}{z_1}\right)+j\theta_{ik}\right] \qquad (89)$$

Now, if $\theta_{ik} = i\alpha_x + k\alpha_y$, Eq (89) becomes "separable",

$$E(U_1(x_1,y_1,t)) = P(x_1,y_1)U_{1s}(x_1,y_1)A\exp\left(-\frac{\sigma^2}{2}\right)\sum_{ik}\sum$$

$$\exp\left(ji(\frac{2\pi}{\lambda})D(\frac{x_1}{z_1}+\frac{\lambda\alpha_x}{2\pi D})\right)$$

$$\exp\left(jk(\frac{2\pi}{\lambda})d(\frac{y_1}{z_1}+\frac{\lambda\alpha_y}{2\pi d})\right) \qquad (90)$$

In spherical coordinates, $x_1 = z_1\sin\psi\cos\zeta$ and $y_1 = z_1\sin\psi\sin\zeta$ where ψ is the angle off of the normal to the array and ζ is the angle in the plane of the array (Fig. 11). The result is the same as in Ref 10:36 (see also Ref 5:141-142, 172-173). Therefore, for a symmetric distribution of lasers around the center of the array and with a

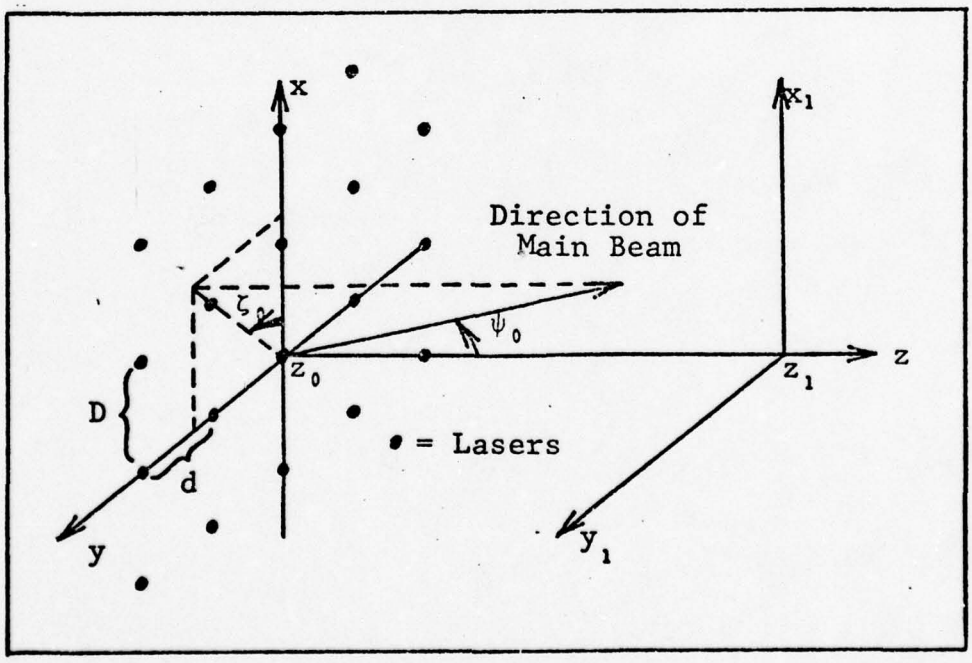

Fig. 11. Geometry of Planar Array and Far Field

laser at the center of the array (i.e. an odd number of lasers in both rows and columns which would require at

least 9 lasers) the pointing angle of the main beam is at ψ_0, ζ_0 where (Ref 10:38)

$$\tan \zeta_0 = \frac{\alpha_y}{\alpha_x} \frac{D}{d} \tag{91}$$

$$\sin^2 \psi_0 = \left(\frac{\lambda}{2\pi}\right)^2 \left(\frac{\alpha_x^2}{D^2} + \frac{\alpha_y^2}{d^2}\right) \tag{92}$$

A conical scan is useful for tracking applications. In terms of ψ_0, ζ_0 a conical scan would require a constant ψ_0 and a ζ_0 that increases linearly with time. If D = d, then

$$\begin{aligned} \alpha_x &= r\cos 2\pi f_s t \\ \alpha_y &= r\sin 2\pi f_s t \end{aligned} \tag{93}$$

will produce a conical scan at a rate of f_s. For this case, $\psi_0 = \sin^{-1} \frac{\lambda r}{2\pi D}$ and $\zeta_0 = 2\pi f_s t$. Because of the grating lobes, the resulting scan in the x_1, y_1 plane will look like a series of concentric circles with amplitudes determined by the overall gaussian envelope.

Aperiodic Arrays

As noted earlier, the grating lobes may not be objectionable depending on the application. However, they must be removed to obtain the resolution inherent in x_p and to eliminate ambiguities in target location due to the numerous lobes. The most feasible way to remove them is to use an aperiodic array where $D_i \neq iD$. The analysis here is similar to radar antenna theory (Ref 5, 30, 35) except that the

wavelengths are much shorter. In general, aperiodic arrays can be designed with the element spacings chosen according to an algorithm or chosen in a completely random manner. The statistics for an ensemble of random array configurations lead to various descriptions of the far field beam pattern. Both types of aperiodic arrays are discussed briefly with general results drawn from antenna theory and applied to the laser case.

Spatial Taper. Unfortunately there is no general theory governing the design of aperiodic arrays. Several techniques are listed in Ref 35:135; the most successful of which is apparently a process called dynamic programming which is a sophisticated trial-and-error procedure. Iterative methods have also been used to synthesize a desired pattern (Ref 36). Ref 20 showed that for a linear array, the lowest side lobe levels were generally from space tapered arrays. Spatial tapering usually results in an array in which the radiating elements are closely spaced near the center of the array and become more spread out near the edge of the array. For example, the element spacings can be made inversely proportional to the aperture excitation (which is considered continuous over the entire array aperture) (Ref 35:126-129). The result is a radiation pattern whose main beam and first couple of side lobes approximate the design goals fairly closely. However, the side lobes tend to get higher for angles further from the main beam (Ref 35:130). Fig. 12 on the next page is a representation of the radiation pattern

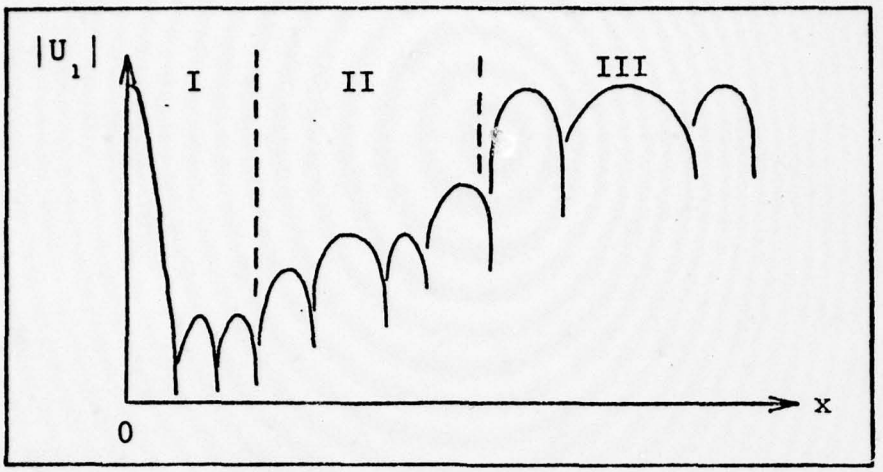

Fig. 12. Representation of Typical Space Tapered Array Pattern (Adapted from Ref 35:130).

for a typical spatially tapered array. Region I approximates the design goals with low side lobes. Region II is a transition region where the side lobes get higher. Region III has average side lobe levels similar to the results for random arrays. If the pattern in Regions II and III will not be used, then perhaps spatial tapering can eliminate the grating lobe problem. In the case of optical frequencies, this might be true because the overall gaussian envelope severely attenuates the pattern away from the main beam. For example, at a distance of $4w_1$ from $x_1 = 0$, the gaussian profile is about 36 db down from the peak at $x_1 = 0$. Unfortunately, because of the small wavelength involved, Region III occurs much closer to the main beam than for the radio frequency case. In fact, for most spatial tapers, the design pattern approaches the Region III results by the first side lobe (Ref 35:150). Since the location of the first side lobe is proportional to $\frac{\lambda}{L}$ where L is the overall length of

the array, the gaussian envelope will not be selective enough in the neighborhood of the main beam to kill off the high side lobes in Regions II and III.

Random Arrays. Strictly speaking there is no such thing as a random array since any physical array is completely deterministic (not including measurement errors). This seems to imply that to determine anything about the far field pattern of an infinitely large class of specific array configurations, one must realize each array and compute its pattern. Fortunately this is not the case. It is possible to make certain probabilistic statements that are valid for such a class of arrays whose elements may be positioned in some random manner. Such statements, though, are merely existence statements or bounds in that, within the class of arrays being considered, at least some array configurations exist whose patterns are described by these probabilistic statements. This approach is absolutely no help at all in realizing a specific array with the desired characteristics. Such a realization must be left to a computer or a designer's insight. Nevertheless, it is useful to review the results of random array analysis (Ref 19, 20, 30, 35).

Eq (50) was the result for the general one dimensional linear array where $\phi_1(t)$ and D were considered gaussian random variables. When considering the far field pattern, the time of observation is arbitrary and will be set to zero so is ϕ_1. Eq (50) becomes,

$$E\{U_1(x_1,y_1,t)\} = P(x_1,y_1)U_{1s}(x_1,y_1)\exp\left[-\tfrac{1}{2}\left(\sigma_\phi^2+\left(2\pi\frac{x_1}{\lambda z_1}\right)^2\sigma_D^2\right)\right]\sum_i$$

$$A_i\exp\left[j\frac{2\pi D_i x_1}{\lambda z_1}\right] \qquad (94)$$

where the D_i are the means of the element locations, and σ_D^2 is their variance (since they are considered to have identical variances). If the array is uniform ($D_i = iD$), the series in Eq (94) has the spatial grating lobes shown in Fig. 8. It can be seen immediately that for $x_1 \neq 0$, σ_D^2 can be appropriately chosen to attenuate the grating lobes. In Eq (51), σ_D was chosen small so that the far field pattern was not significantly affected; here, however, $\left(2\pi\frac{x_1}{\lambda z_1}\sigma_D\right)^2$ must be relatively large to accomplish the desired result. In a manner completely analagous to the temporal results of Eqs (34) and (35), the mean far field intensity is proportional to N for $x_1 \neq 0$ since

$$E\{I_1\} \propto \left[1-\exp\left(\left(2\pi\frac{x_1}{\lambda z_1}\right)^2\sigma_D^2\right)\right]N + \exp\left(\left(2\pi\frac{x_1}{\lambda z_1}\right)^2\sigma_D^2\right)\left[\frac{\sin N\pi D\frac{x_1}{\lambda z_1}}{\sin \pi D\frac{x_1}{\lambda z_1}}\right]^2 \qquad (95)$$

where $A_i = A$ and $D_i = iD$ in Eq (94). At $x_1 = 0$, however, the main beam peak is proportional to N^2. Therefore, the power ratio of the average side lobe level to the main beam peak is $\frac{N}{N^2} = \frac{1}{N}$, so that the average side lobe level is inversely proportional to the number of lasers in the array (Ref 35:140-142).

There is still, however, a finite probability that some side lobe will be much higher than the average side lobe level of $\frac{1}{N}$. This is true since the far field pattern of any given array is simply one possible sample function of all of those under consideration, and any individual sample function may have very high or very low side lobes. Eq (94) indicates that the mean of U_1 can be made to attenuate the grating lobes for $x_1 \neq 0$ as much as desired. The field, however, may deviate from this mean by a considerable amount. To investigate this deviation a new definition is used so that the field under consideration is zero mean and unit variance

$$U_1'(x_1,y_1,t) = \frac{U_1(x_1,y_1,t) - E\left(U_1(x_1,y_1,t)\right)}{\sqrt{\mathrm{Var}\left(U_1,U_1^*\right)}} \qquad (96)$$

In general, U_1' is a complex random process with real and imaginary parts. For a large number of elements, these parts may be considered asymptotically jointly gaussian random processes by the central limit theorem (Ref 19:258; 35:147). With this assumption, the joint probability density of the real and imaginary parts of the field U_1' is known, and the probability that any side lobe (a given amplitude of the field) will not exceed some specified threshold can be determined. (This is not the same as the assumption that was made earlier that only the statistics of the phase were known and that the amplitude was deterministic. In this case, both the amplitude and phase of

the far field U_i' are considered random for this class of arrays since the elements may have locations determined by some unspecified probability density.) Since U_i' is zero mean, its real and imaginary parts are identically distributed as well as independent. This is because the element locations are considered to have a common underlying probability density, so that the element positions are identically distributed about their means D_i. Now $\mathrm{Var}(U_1 U_1^*) = N$ from Eq (95) since $E(I_1) = E(U_1 U_1^*) = \mathrm{Var}(U_1 U_1^*)$ and σ_D^2 is big enough. Following Ref 19:261 and 35:147-151, the result is as follows:

$$\Pr\left(|U_1'| > \frac{A_0}{\sqrt{N}}\right) = 1-\Pr\left(|U_1'| < \frac{A_0}{\sqrt{N}}\right)$$

$$= \exp\left(-\frac{A_0^2}{N}\right)$$

$$\Pr\left(|U_1'|^2 > \frac{A_0^2}{N}\right) = \exp\left(-\frac{A_0^2}{N}\right)$$

$$\Pr\left(|U_1'|^2 > B\right) = \exp(-B) \qquad (97)$$

where $B = \frac{A_0^2}{N}$ is the power ratio of the desired threshold to the average side lobe level. The exponential dependence is obtained from the exponential distribution of the amplitude of $|U_1'|$. The probability that the peak side lobe is less than B is just $1-e^{-B}$. Eq (97), however, is true for only a single sample value of U_1' at some x_1. To find the

probability that no side lobe anywhere in the pattern exceeds B, it is necessary to take many spatial samples of U_1'. The issue now is how many samples should there be and where should they be. The latter problem is reduced by simply choosing the distance between samples to be the same. To make the computations simpler, the number of samples may be constrained by the requirement that the samples be statistically independent. Crudely, then, the number of samples needed to describe the random process is a set of independent random variables. For such a case, the samples are separated by no less than the coherence distance of the pattern and the pattern is considered piecewise constant over a coherence length. The total probability that the set of $\{|U_1'(x_i)|\}$ is less than B is just the product of the probabilities that each individual sample is less than B,

$$\begin{aligned}\beta &= \Pr\left(\{|U_1'(x_i)|^2\}<B\right) \\ &= \Pr\left(|U_1'(x_1)|^2<B \text{ and } |U_1'(x_2)|^2<B \text{ and...} |U_1'(x_n)|^2<B\right) \\ &= (1-\exp(-B))^n \end{aligned} \tag{98}$$

where n is the number of samples and is called the array parameter. As the coherence distance of the pattern gets small, n gets large. Eq (98) can be rewritten,

$$B = -\ln\left[1 - \beta^{\frac{1}{n}}\right] \tag{98a}$$

Now if the probability (confidence level) β is chosen and n is known, then the peak side lobe level (with respect to

the average side lobe level, $\frac{1}{N}$), B, can be determined. For example, for a 90% probability that no side lobe exceeds B and for n = 10, then B = 4.56, i.e. with 90% confidence, the peak side lobe of $|U_1'|^2$ is 4.56 times as high as the average side lobe level, $\frac{1}{N}$. It should be noted, too, that the underlying distribution of the array element locations is not a factor in this analysis; this is one of the reasons why the analysis is general for a large class of array configurations.

The determination of the array parameter, n, can be made in several ways (Ref 35:151-156) and the result can be given by

$$n = \frac{L}{\lambda} \tag{99}$$

where L is the length of the array. This is intuitively correct since $\frac{\lambda}{L}$ is roughly the angular lobe width of the pattern, therefore the necessary "sample rate" should be proportional to $\frac{\lambda}{L}$. For optical wavelengths, then, (particularly for CO_2 lasers) n is on the order of 10^5. The effects on n of a main beam at some location other than $x_1 = 0$, unequal element excitations, non-isotropic elements, and signal bandwidth are all negligible (to within an order of magnitude) for this case (Ref 35:171-184).

Eq (98) overlooked a minor problem. Since B itself has a variance and the samples are not infinitely close together (continuous), the actual peak side lobe is higher than B with probability one, i.e. U_1' may not be piecewise

constant over a coherence distance. Ref 19 ignores the error and Ref 35 presents a rather obtuse derivation of an additive correction factor which turns out to be $1 + \frac{2}{B}$, so that the actual peak side lobe is given by $B + 1 + \frac{2}{B}$. For the optical wavelengths, the correction factor is negligible, since $n = 10^5$ and Eq (98a) gives $B \approx 12$ (for a confidence level of 50%) and $B \approx 14$ (for $\beta = 90\%$). Thus, the correction affects the actual peak side lobe less than about 10% numerically, and in fact merely represents a small decrease in the confidence level β. Since B is the ratio of the peak side lobe to the average side lobe, the ratio of the peak side lobe to the main beam is given by

$$h = \frac{B}{N}$$

$$= -\frac{1}{N} \ln\left(1 - \beta^{\frac{1}{n}}\right) \qquad (100)$$

The primary restriction on Eq (100) results from the original assumption that the field U_1' had real and imaginary parts that were asymptotically jointly gaussian. Ref 19:262 notes that this approximation is valid for $\frac{\sqrt{N}}{\pi h^3} << 1$. A plot of N versus h is given in Fig. 13 for q = 1,5 where $L = 10^q\lambda$ and $\beta = 90\%$. The restriction $\frac{\sqrt{N}}{\pi h^3} << 1$ is shown by a dotted line. Left of this line, the confidence level may be less than 90%. The figure is very nearly the same as that in Ref 19:262. The figure indicates that as L(q) increases, the peak side lobe is also likely to increase, but not a great deal relatively.

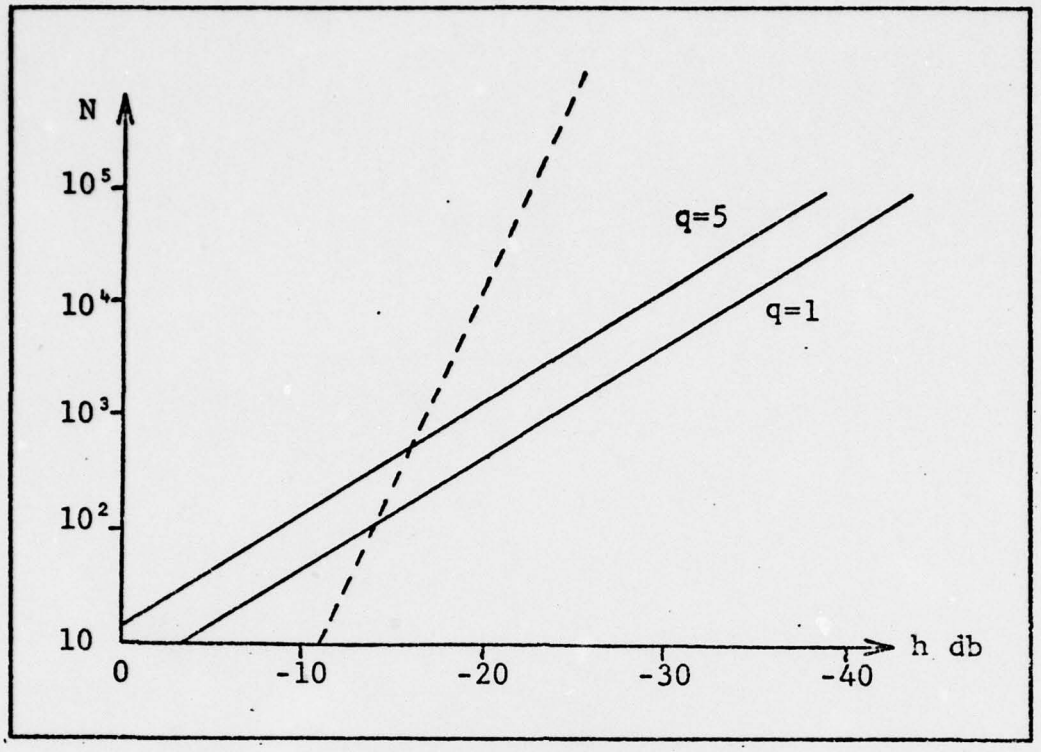

Fig. 13. Peak Side Lobe Level Versus N.

Fig. 13 also indicates a very striking result. For a reasonable peak side lobe level of -20 db, a 1 m array ($q \approx 5$) must consist of about 1400 lasers. As noted earlier, these probability statements are existence statements for an infinitely large class of arrays whose elements are positioned according to some underlying probability density. Therefore, there are at least some arrays which have about 1400 lasers whose side lobes are less than -20 db with a confidence level of about 90%. This is not true for most of the arrays in the class. Furthermore, this is not a design procedure for a specific array. Finding an array with the above performance is by no means a trivial task (analytically, it is totally intractable). However, even disregarding the difficulty of

designing the appropriate array, there is the not inconsiderable problem of actually building it.

V. Conclusion

Summary of Results

In the first section, classical, amplitude stabilized fields were used to describe the laser output. The fields were considered complex, coherence separable random processes. The Huygens-Fresnel principle was used to propagate the field, and the far field (Fraunhofer condition) was considered. The general result for the superposition of N fields contained all of the cases discussed, and the time-space duality of the calculations was evident. When coherent detection was used to measure a field at any space-time point, the resulting measured phases of the fields were considered stationary, gaussian random processes. The effect on the far field pattern was an amplitude reduction proportional to the variance of the phase. As the variance increased, the result approached the incoherent case; and as the variance approached zero, the fields were seen to add coherently. A phase locked loop was postulated to lock each laser to a reference. A local oscillator could be used in a coherent (heterodyne) detector, and a phase locked loop could lock the reference to the local oscillator. The receiver then could track the signal without regard to the absolute phase variations of the signal or the local oscillator. Three cases of misalignment were considered. Variations in laser spacing produced results similar to the effect of the phase variance. In each case the required standard deviation for a desired effect on the far field was determined. Misalignment of the

laser axes was also considered and found to require alignment accuracy to within milliradians for the coaxial case. One other problem investigated was that of the misalignment of the fields in the direction of propagation. This was seen to produce a non-negligible phase variation in the far field that required physical alignment of the lasers to within an optical wavelength to eliminate the variation. The statistics resulted in another amplitude reduction of the far field proportional to the variance of the misalignment.

A few, minor, simplifying assumptions in the first section produced a far field result almost identical to that of a mode-locked laser. However, there was additional flexibility in that the pulse widths and pulse rates could be easily varied by changing the frequencies of the individual lasers. The minimum pulse width was determined to be about 3 nsec using CO_2 waveguide lasers. A laser array also produced spatial modulation. In both cases the overall beam propagated as a gaussian spherical wave.

In the second section, the case of several lasers whose optical axes were coincident was considered in more detail. For the reasonable assumptions of coherent detection and a matched filter receiver, the performance of the mean of the far field was seen to be described in terms of the ambiguity function. The general characteristics of the ambiguity function depended essentially on the total bandwidth of the combined field. Thus using other than a constant frequency interval Δf would not be significantly helpful. The

measurement precisions for range and velocity were found to be proportional to $\frac{1}{\sqrt{N^3\Delta f}}$ and $\sqrt{N\Delta f^3}$ respectively. Therefore, in theory, the measurement precisions could almost independently be made as small as desired within the constraint that $N\Delta f$ must be less than or equal to the laser gain line width. Multiple pulses could also be used to increase the signal energy to noise ratio thus improving both measurements. Overall modulation such as linear frequency modulation (chirp) was not seen to be particularly useful in improving measurement precision. This coaxial case does have application to target detection and tracking problems as well as terrain mapping. The system is very flexible because of the capability to change pulse characteristics, thus changing measurement precision when necessary.

In the third section, the case of an array of lasers was considered. A linear array was analyzed and found to have a spatial pulse that scanned linearly beneath the overall gaussian envelope. This spatial pulse was seen to require about two orders of magnitude improvement in the alignment accuracy of the optical axes of the lasers, i.e. on the order of 10^{-5} rad. By the use of z transforms, the side lobes of the spatial pulse could be controlled in any desired manner. For the monochromatic case ($\Delta f=0$), the spatial beam could be made to scan sinusoidally and a planar array was seen to permit conical scanning. These results make the system applicable to target tracking and even track-while-scan since the beams' relative phases can be changed

electronically. For some applications, however, the secondary spatial beams, called grating lobes, are undesirable, so the cases of aperiodic and random arrays were considered briefly. Of the aperiodic arrays, the spatial taper was found to provide some of the lowest side lobes, but for optical wavelengths the beam pattern away from the main peak became less controllable. The class of arrays with element locations determined in a random manner from array to array was found to have a ratio of average side lobe intensity to peak intensity inversely proportional to the number of lasers. Furthermore, to obtain a reasonably high probability of low side lobes (i.e. no grating lobes), the array was found to require a large number of lasers (>1000). Although this was noted to be true in general for the class of random arrays, the results only guaranteed that a desirable array existed and did not in any way specify the array.

Recommendations

It is very difficult at this point to make specific recommendations as to what type of system should be built, how many lasers it should use, what frequencies it should operate at, and so on. The difficulty arises because as is usually the case, none of the issues are clear enough to enable instant conclusions to be drawn. As always, there are trade-offs necessary between system requirements, design constraints, and costs. The difficulty becomes even more acute when the applications are generalized as they are here.

and when there are no systems against which point by point comparisons may be made. Nevertheless, some general comments may be made. The statistical models used indicate that given a good phase locked loop design for heterodyne detection, the fields may be combined and detected coherently. Misalignment problems in the plane of the array and in optic axis angle, though difficult, also seem to be within the realm of engineering solutions. The waist alignment problem (in the direction of propagation) is much more serious and may represent the most serious stumbling block to implementing coherent combination of two or more lasers. The flexibility of such a system is desirable for ranging applications and possibly for velocity measurements as well since the pulse format may be changed easily. This would indicate, however, that more than two or a few lasers be used (exactly how many more depends on the system requirements) since the measurement precision for coupled measurements may be more easily manipulated for N>2. The coaxial case requires some sort of combination scheme, however, which may be lossy as well as expensive. A linear array may find application in cases where beam scanning or pointing is necessary. However, unless it is possible to build arrays of more than several hundred lasers within a length of a few meters or less, the multiple lobe problem cannot be eliminated. This will certainly restrict the application of such a system even though the high resolution of the coherent result ($\sim$ cm) may be desirable.

AD-A053 349 AIR FORCE INST OF TECH WRIGHT-PATTERSON AFB OHIO SCH--ETC F/G 20/5
FIELD PROPERTIES OF MULTIPLE, COHERENTLY COMBINED LASERS.(U)
DEC 77 H E HAGEMEIER

UNCLASSIFIED AFIT/GEO/EE/77D-3 NL

2 OF 2
AD
A053349

END
DATE
FILMED
6-78
DDC

There are several areas in which further investigation would be helpful and in which hardware development should be emphasized. The duality issue should be considered more carefully. It appears that not only could more results be obtained, but a great deal of spatial statistics from antenna theory could be applied to the temporal realm. As far as the spatial beam is concerned, there should be further study of the spatial taper case for the optical wavelengths. Either a general theory could be developed or the approach could be shown conclusively to be of little value. Computers would be helpful in determining actual patterns for various arrays to see if there are any useful trends. For the random case, the statistics should be examined more closely to produce more rigorous results. Another interesting possibility is that of developing a measure of the probability that an objectionably high side lobe will occur within a certain region near the main beam. Another area is that of signal design. Some of the performance criteria presented in this study are basic and could be expanded. Signal synthesis would also open up the whole area of applications to communications that were not considered here. It seems that the coherent combination of lasers would have enough more flexibility than a mode-locked laser to be useful in communications. The spatial scanning aspects of the array could also be helpful in, perhaps, selecting various receivers for various messages, i.e. in addition to frequency and time division multiplexing, spatial multiplexing could be useful.

Coherent combination of lasers, although a formidable engineering task, still offers some attractive benefits. Development of arrays of small lasers with power outputs of watts or milliwatts should be encouraged. Laser alignment is enough of a problem that it is desirable to obtain more lasers and more power per laser in a given array. Other hardware problems that must be addressed include the physical aspects of putting a large number of lasers together in a small array with the associated cooling, control electronics, and optics.

Bibliography

1. Aplet, L. J., et al. Laser Array Techniques. Quarterly Progress Letter No. 3A. Culver City, California: Hughes Aircraft Co., 1960. AD 821235.

2. Arecchi, F. T. and A. Berné. "High-Order Fluctuations in a Single Mode Laser Field." Physical Review Letters, 16:32-35 (January, 1966).

3. Arutyunyan, A. G., et al. "Spatial Field and Intensity Correlation Functions of Laser Radiation." Soviet Physics - JETP, 37:764-771 (November, 1973).

4. Born, M. and E. Wolf. Principles of Optics. New York: Pergamon Press, 1975.

5. Collin, R. E. and F. J. Zucker. Antenna Theory Part I. New York: McGraw-Hill, 1969.

6. Cook, C. E. and M. Bernfeld. Radar Signals. New York: Academic Press, 1967.

7. Corcoran, V. J. "Far-Infrared--Submillimeter Phased Arrays and Applications." IEEE Transactions on Microwave Theory and Techniques, 22:1103-1107 (December, 1974).

8. Cutler, L. S. and C. L. Searle. "Some Aspects of the Theory and Measurement of Frequency Fluctuations in Frequency Standards." Proceedings of the IEEE, 54: 136-154 (February, 1966).

9. Degnan, J. J. "The Waveguide Laser: A Review." Applied Physics, 11:1-33 (November, 1976).

10. Elliot, R. S. "The Theory of Antenna Arrays." Microwave Scanning Antennas Vol. II, edited by R. C. Hansen. New York: Academic Press, 1966.

11. Gagliardi, R. M. and S. Karp. Optical Communications. New York: John Wiley and Sons, 1976.

12. Goodman, J. W. Introduction to Fourier Optics. New York: McGraw-Hill, 1968.

13. Goodman, J. W. "Statistical Properties of Laser Speckle Patterns." Laser Speckle and Related Phenomena, edited by J. C. Dainty. New York: Springer-Verlag, 1975.

14. Harrington, R. F. Time-Harmonic Electromagnetic Fields. New York: McGraw-Hill, 1961.

15. Hecht, E. and A. Zajac. Optics. Reading, Massachusetts: Addison-Wesley, 1974.

16. Komai, L. G., et al. Multi-Laser Element Techniques. AFAL TR 66-134. Wright-Patterson Air Force Base, Ohio: Air Force Avionics Laboratory, 1966.

17. -----. Laser Array Techniques. AFAL TR 66-257. Wright-Patterson Air Force Base, Ohio: Air Force Avionics Laboratory, 1966.

18. Lamb, W. E. "Theory of Optical Masers." Quantum Optics and Electronics, edited by C. DeWitt, et al. New York: Gordon and Breach, 1965.

19. Lo, Y. T. "A Mathematical Theory of Antenna Arrays with Randomly Spaced Elements." IEEE Transactions on Antennas and Propagation, 12:257-268 (May, 1964).

20. Lo, Y. T. and S. W. Lee. "A Study of Space Tapered Arrays." IEEE Transactions on Antennas and Propagation, 14:22-30 (January, 1966).

21. Mandel, L. and E. Wolf. "Coherence Properties of Optical Fields." Reviews of Modern Physics, 37:231-284 (April, 1965).

22. Mangulis, V. Handbook of Series for Scientists and Engineers. New York: Academic Press, 1965.

23. Middleton, D. An Introduction to Statistical Communication Theory. New York: McGraw-Hill, 1960.

24. Minkowski, J. M. and C. J. Gundersdorf. Quantum Limitations on Optical Communications. AFAL TR 71-58. Wright-Patterson Air Force Base, Ohio: Air Force Avionics Laboratory, 1971. AD 882879.

25. Oppenheim, A. V. and R. W. Schafer. Digital Signal Processing. Englewood Cliffs, New Jersey: Prentice-Hall, 1975.

26. Papoulis, A. Probability, Random Variables, and Stochastic Processes. New York: McGraw-Hill, 1965.

27. -----. Systems and Transforms with Applications in Optics. New York: McGraw-Hill, 1968.

28. Pincinbono, B. "Statistical Properties of Randomly Modulated Laser Beams." Physical Review A, 4:2398-2407 (December, 1971).

29. Pincinbono, B. and E. Boileau. "Higher-Order Coherence Functions of Optical Fields and Phase Fluctuations." Journal of the Optical Society of America, 58: 784-789 (June, 1968).

30. Richards, W. F. and Y. T. Lo. "Antenna Pattern Synthesis Based on Optimization in a Probabilistic Sense." IEEE Transactions on Antennas and Propagation, 23:165-172 (March, 1975).

31. Rihaczek, A. W. Principles of High Resolution Radar. New York: McGraw-Hill, 1969.

32. Rowe, H. E. Signals and Noise in Communications Systems. New York: D. Van Nostrand, 1965.

33. Siegman, A. E. An Introduction to Lasers and Masers. New York: McGraw-Hill, 1971.

34. Siegman, A. E., et al. "Preliminary Measurements of Laser Short-Term Frequency Fluctuations." IEEE Journal of Quantum Electronics, 3:180-189 (May, 1967).

35. Steinberg, B. D. Principles of Aperture and Array System Design. New York: John Wiley and Sons, 1976.

36. Stutzman, W. L. and E. L. Coffey. "Radiation Pattern Synthesis of Planar Antennas Using the Iterative Sampling Method." IEEE Transactions on Antennas and Propagation, 23:764-769 (November, 1975).

37. Van Trees, H. L. Detection, Estimation, and Modulation Theory Part III. New York: John Wiley and Sons, 1971.

38. Viterbi, A. J. Principles of Coherent Communications. New York: McGraw-Hill, 1966.

39. Yariv, A. Quantum Electronics (Second Edition). New York: John Wiley and Sons, 1975.

40. Ziemer, R. E. and W. H. Trantor. Principles of Communications. Geneva, Illinois: Houghton Mifflin, 1976.

41. Hayes, C. L. and L. M. Laughman. "Generation of Coherent Optical Pulses." Applied Optics, 16:263-264 (February, 1977).

Vita

Hal E. Hagemeier, 27, is from Houston, Texas. He graduated with highest honors from the University of Texas at Austin in 1972 with a Bachelor of Science in Electrical Engineering. He is a Distinguished Military Graduate of AFROTC and is a member of Tau Beta Pi, Eta Kappa Nu, Phi Kappa Phi, Phi Eta Sigma, and Omicron Delta Kappa. Before entering the Air Force in October 1972, he worked as an engineer with Exxon Company, USA in Houston. He entered active duty as a Developmental Electronics Engineer at Offutt Air Force Base and was assigned to the ELINT Exploitation Branch of the 544th Intelligence Exploitation Squadron. His responsibilities included the analysis of scientific and technical ELINT data, evaluation of ELINT collection systems and ground processing equipment, preparation of special studies for the SAC staff, and assistance to other organizations in the U. S. intelligence and electronic warfare communities. He entered the School of Engineering, Air Force Institute of Technology, in June 1976.